2009

Individual copper nanowire decorated by gold nanoparticles for Surface enhanced Raman scattering

Roshan Guttikonda
University of Nevada Las Vegas

INDIVIDUAL COPPER NANOWIRE DECORTAED BY GOLD NANOPARTICLES FOR SURFACE ENHANCED RAMAN SCATTERING

by

Roshan Guttikonda

Bachelor of Technology
Acharya Nagarjuna University, Guntur
2007

A thesis submitted in partial fulfillment

of the requirements for the

Master of Science in Electrical Engineering
Department of Electrical and Computer Engineering
Howard R. Hughes College of Engineering

Graduate College
University of Nevada, Las Vegas
December 2009

UNLV
UNIVERSITY OF NEVADA LAS VEGAS

THE GRADUATE COLLEGE

We recommend that the thesis prepared under our supervision by

Roshan Guttikonda

entitled

Individual Copper Nanowire Decorated by Gold Nanoparticles for Surface Enhanced Raman Scattering

be accepted in partial fulfillment of the requirements for the degree of

Master of Science
Electrical Engineering

Biswajit Das, Committee Chair

Yingtao Jiang, Committee Member

Mei Yang, Committee Member

Laxmi P. Gewali, Graduate Faculty Representative

Ronald Smith, Ph. D., Vice President for Research and Graduate Studies
and Dean of the Graduate College

December 2009

ABSTRACT

Individual Copper Nanowire Decorated by Gold Nanoparticles for Surface Enhanced Raman Scattering

by

Roshan Guttikonda

Dr. Biswajit Das, Examination Committee Chair
Professor of Electrical Engineering
University of Nevada, Las Vegas

In this Thesis, I discuss the theory, implementation and applications of Surface enhanced Raman scattering (SERS). Surface enhanced Raman scattering has been used to detect 4 mercaptopyridine molecules. On a Silicon wafer, Gold nanoparticles are deposited onto Copper nanowires. Hotspots occur at the small gap (less than 10nm) between the nanowire and nanoparticle. The interaction of the electromagnetic field of the incident laser and the surface plasmon resonances of the metal nanoparticles at the hot spots enhances the Raman scattering signal of the adsorbed pyridine molecule ($10^{-3}M$). The dependence of SERS signal on the polarization angle of the incident laser is observed. When compared to other SERS substrates (gold, silver) this one is very economical.

ACKNOWLEDGEMENTS

First and foremost I offer my sincere gratitude to my advisor Dr. Biswajit Das, who has supported me throughout my studies at UNLV, giving me the room to work in my own way. One simply could not wish for a better advisor.

His passion for nanotechnology has always inspired me. His research experience and teaching of Semiconductor concepts has helped me to understand them in a better way. I would like to thank Dr. Qian Lihua for helping me with the Copper electroplating, SEM imaging, Raman Spectroscopy of the samples. I would like to thank Wen Shen and Neel for their help in the lab. I would like to thank my committee members Dr. Mei Yang, Dr. Yingtao Jiang, Dr. Laxmi P. Gewali for their suggestions.

Finally I would like to thank my parents Sri Ram Murthy, Padma and my brother Pradeep for their love and affection.

TABLE OF CONTENTS

LIST OF FIGURES

CHAPTER 1

INTRODUCTION

1.1 Thesis outline and chapter overview

In this Thesis, I discuss the theory, implementation and applications of Surface enhanced Raman scattering (SERS). Surface enhanced Raman scattering has been used to detect 4 mercapto pyridine molecules. Very small concentrations of pyridine molecules are used for detection. On a Silicon wafer, Gold nanoparticles are deposited onto Copper nanowires. Hotspots occur at the small gap (nm) between the nanowire and nanoparticle. The interaction of the electromagnetic field of the incident laser and the surface plasmon resonances of the metal nanoparticles at the hot spots enhances the Raman scattering signal of the pyridine molecule ($10^{-3}M$). The dependence of SERS signal on the incident polarization is performed. SERS has been successfully performed using gold and silver substrates by many groups. When compared to other SERS substrates (gold, silver) this one is very economical.

Chapter 2 provides the theoretical background of Anodization, Electrodepositon, Atomic layer deposition and the experimental procedure in which the Copper nanowires are obtained by electroplating the anodized porous alumina. The experimental procedure in which the gold nanoparticles are prepared is also described.

Chapter 3 provides the theory of Raman scattering, Surface enhanced Raman scattering and their applications. The complexities involved with SERS over Raman scattering are also discussed.

Chapter 4 discusses Real life applications of SERS.

Chapter 5 provides the effect of electromagnetic enhancement in the absence of adsorbed molecule, the effect of isolated nanoparticles vs aggregate nanoparticles is described, Influence of geometry on SERS, influence of polarization on SERS intensity are described in detail

Chapter 6 shows the experimental results for SERS on Silicon wafer, surface has copper nanowires decorated by gold nanoparticles for detection of 10^{-3}M ethanol 4 mercapto pyridine molecules. The experimental results of the polarized SERS response for the substrate prepared are presented.

CHAPTER 2

FABRICATION OF COPPER NANOWIRES AND GOLD NANOPARTICLES

2.1 Introduction

The fabrication of Copper nanowires is done by electroplating Copper into PAA (Porous Anodic Alumina) and then the Porous Alumina layer is removed to get the nanowires. Strong electromagnetic coupling is obtained at the junction between the copper nanowires and gold nanoparticles which is responsible for the SERS.

2.2 Anodization

Anodization is the process of growing an oxide layer by electrochemical process on certain metals like aluminum, niobium, tantalum, titanium, tungsten, and zirconium. Each metal has a different growth condition for the oxide layer. The thickness and its properties depend on the metal. Of these the oxides of aluminum and tantalum have commercial and technological applications. The unique property of Aluminum among these metals is that, along with the thin barrier oxide, a thick oxide coating will be formed by anodizing aluminum alloys in certain acidic electrolytes, which contain high density of microscopic pores. This porous coating is a product of anodizing.

In an anodizing cell, the aluminum will be the anode which is connected to the positive terminal and the cathode to the negative terminal of the DC power supply. The cathode should be an electronic conductor that will be inert in the anodizing bath like carbon, lead, stainless steel, and nickel. When the circuit is closed, the electrons from the metal are attracted by the positive terminal and at the metal surface ions react with water

to form an oxide layer. Then the electrons get back to the electrolyte at the cathode and react with hydrogen ions and hydrogen gas is released.

Electrolytes used for Anodization are selected so that the oxide is insoluble, or the oxide growth rate is higher than the deposition rate thereby we can get a net oxide layer. The electrolyte composition decides if the film will be barrier or porous. If we use near neutral solutions we get barrier oxide because aluminum oxide is not soluble in it, most commonly used electrolytes are ammonium borate, phosphate, or tartrate compositions[1]. Porous oxide is obtained in acid electrolytes in which oxide will not only be deposited, but also dissolves. We will be dealing with porous oxide layers.

2.2.1 Porous anodic oxides

Dilute sulfuric acid is the most commonly used electrolyte to grow porous aluminum oxides, typically 10 weight% concentration. Other electrolytes like phosphoric acid, chromic acid, oxalic acid are also used for some commercial applications. All these electrolytes are capable of retaining high concentration of aluminum in the solution so that the aluminum that is oxidized is not on the film but in the solution. For example, when alumina is anodized in sulfuric acid, 60% of the oxidized aluminum is in the film and the remaining is in solution. Porous films with a thickness of 100 μm can be made easily. Even the thickest barrier films will be 100 times thinner than porous films. Barrier films require a high voltage but porous films do not require the high voltage.

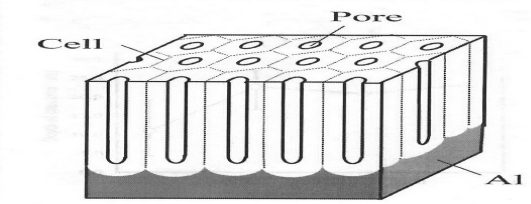

Fig 2.1 Idealized structure of anodized porous alumina

The oxide contains a cellular structure with a central pore in each cell. In fig 2.1 we can see the uniform hexagonal cells, but in normal Anodization conditions the films we get will not be periodically aligned. The deciding factors for the cell and pore dimensions are electrolyte composition, temperature, and voltage. However for any of the possible conditions in the end we get high density of pores. The cell diameter is in the range 50-300 nm and the pore diameter is typically 1/3 to 1/2 of the cell diameter. The cell population density varies from approximately 10 to more than 100 per μm^2. The aspect ratio is commonly of the order of 1000:1. For example, coatings grown in sulfuric acid usually have a film thickness of 20 to 50 µm with 20 nm pores[1].

2.2.2 Anodization reactions

The overall reaction that takes place during Anodization is [1]:

$2Al + 3H_2O \Longrightarrow Al_2O_3 + 3H_2$ [2.1]

This is the sum of the separate reactions at each electrode. The reactions at the anode occur at the metal/oxide and oxide/electrolyte interfaces. The ions that make up the oxide move fast under the high field conditions. At the metal/oxide interface the oxygen anions react with the metal:

$2Al + 3O^{2-} \Longrightarrow Al_2O_3 + 6e^-$ [2.2]

At the oxide/electrolyte interface outward moving aluminum cat ions react with water:

$2Al^{3+} + 3H_2O$ ==> $Al_2O_3 + 6H^+$ [2.3]

While the aluminum dissolution into the electrolyte happens during porous film formation, the reaction at the anode is:

2Al ==> $2Al^{3+} + 6e^-$ [2.4]

Then at the cathode, hydrogen gas is released:

$6H^+ + 6e^-$ ==> $3H_2$ [2.5]

2.2.3 Whatmann Anodisc

We used a commercially available anodisc from Whatmann. The pore size is $0.02\mu m$ and diameter of the anodisc is 13mm.

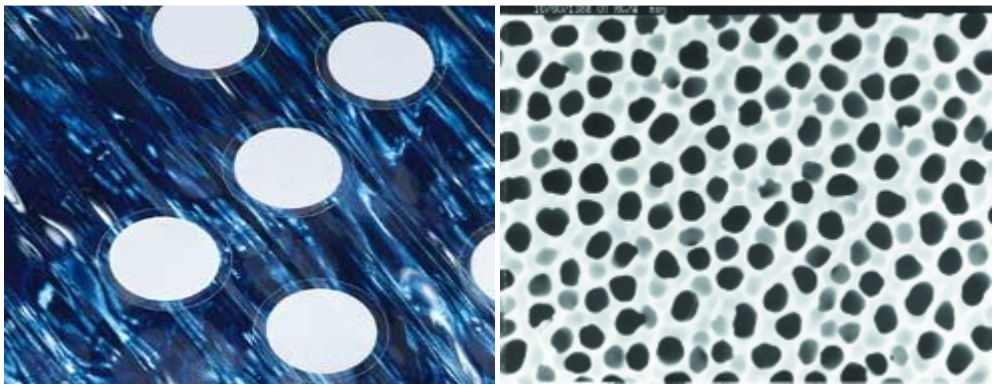

Fig 2.2 Anopore disc and pore alignment

The Anopore inorganic membrane (Anodisc™) has a wide range of laboratory filtration applications. This highly ordered material has a precise, non deformable honeycomb pore structure with no lateral crossovers between the individuals. The

Anopore inorganic membrane is characterized by high purity alumina matrix manufactured electrochemically.

The precise pore structure and narrow pore size distribution of the Anopore membrane ensure a higher efficiency of particle removal. Microorganisms and particulate material are captured on the surface of the membrane for subsequent analysis by light or electron microscopy. If the membrane is wet it is virtually transparent, i.e. microscopic examination of the retained particles can be performed on the same surface.

The porous membrane is hydrophilic and compatible with most solvents and aqueous materials. As no monomers, plasticizers, adhesives, surfactants or wetting agents are used in the manufacturing process, it prevents sample contamination is prevented and low protein binding and minimal loss of sample is ensured.

The commercial Anopore membrane supplied by Whatmann will be in the form of Anodisc membrane filters. The membrane is peripherally bonded to an annular polypropylene ring for ease of handling and is suitable for both vacuum and pressure filtration.

Anopore is supplied in 3 nominal pore sizes: 0.02 µm, 0.1 µm, and 0.2 µm, and in 3 diameters: 13 mm, 25 mm, and 47 mm^2.

2.3 Sputtering

Sputtering is a method which involves depositing thin films of a material onto a surface. First gaseous plasma is created and then the ions are accelerated from the plasma to a source material. As a result the source material will be eroded by the arriving ions by energy transfer and it is ejected in the form of neutral particles, i.e. either individual

atoms, clusters of atoms or molecules. When the neutral particles are ejected they will travel in a straight line till they come into contact with something like other particles or a nearby surface. If a substrate such as a Porous Alumina disc is placed in the path of these ejected particles, the anodisc will be coated by a thin film of the source material (Au)[3].

2.3.1 Powering the electrode with DC Voltage

1) Ever present "free electrons" will immediately be accelerated away from the negatively charged electrode (cathode). These accelerated electrons approach the outer shell electrons of neutral gas atoms in their path and, being of a like charge; will repel the electrons off the gas atoms. The gas atom becomes electrically unbalanced since it will have more positively charged protons than negatively charged electrons, thus it is no longer a neutral gas atom but a positively charged 'ion'(e.g. Ar +).
2) At this point of time the positive ions accelerate into the negatively charged electrode, (cathode) striking the surface and blasting loose electrode material (diode sputtering) and more free electrons by energy transfer. The extra free electrons feed the formation of ions and the plasma is continued.
3) Free electrons always try to get back to the outer electron shells of the ions and change them back into neutral gas atoms. As per the law of conservation of energy, when these electrons return to a ground state, the resultant neutral gas atom gains energy and the energy is released in the form of a photon. As the photons are released the plasma keeps glowing.

2.3.2 Sputter Coater

Fig 2.3 SPI module sputter coater

We used the SPI module sputter coater. It has two components

1) SPI module control
2) SPI module sputter coater

The SPI-MODULE CONTROL unit has been designed as the basis of a range of SEM sample coating instruments. The main cabinet contains all the necessary hardware to control and monitor vacuum pressure within the work chamber.

The SPI-SPUTTER COATER with Etch Mode Module is a sputtering power supply generating more than 1000 volts DC consisting of a diode magnetron sputtering head and a 3MIL gold cathode[4].

2.3.3 Thickness of coating

A thickness of 100-300 angstroms can be obtained. The thickness of the coating can be obtained from the equation

$$d = K\ I\ V\ t \qquad [2.6]$$

Where

‘d’ is the thickness of the coating in angstroms

‘K’ is an experimental constant depends on the metal being sputtered, gas, 5cm distance between the target and specimen

‘I’ is the plasma current

‘V’ is voltage applied in kilovolts

‘t’ is sputtering time in seconds

For our experiment K=0.17 (gold used in conjunction with Argon), plasma current of 18 mA and sputtering time of 120s

$$d = 0.17 \times 18 \times 1 \times 120 = 367 \text{ angstroms}$$

The thickness also depends on the cleanliness of the sputtering system.

2.3.4 Experimental Section

1) The porous alumina is loaded on to the specimen holder
2) The glass work chamber and the sputter head are put back in their places
3) The leak valve is fully closed and the argon pressure is set to 5psi
4) When the SPI module control is turned on, the rotary pump will start immediately and after 10-15 seconds the vacuum gauge will let the pressure inside the chamber drop to 600 millitorr (approx)
5) The gas leak valve is opened partially to flush the work chamber with argon for 15 seconds. Closing the leak valve we wait for the pressure inside the work chamber to drop to 80 millitorr.
6) The sputter coater is turned on
7) The gas leak valve is again opened until the pressure just begins to rise and by pressing the test button and by adjusting the leak valve, set the plasma current to 18 mA. A visible discharge will be observed in the chamber

8) On the sputter coater select the sputter mode and set the sputter time to 120s and press the start button
9) After the plasma extinguishes turn off both power supplies and vent the chamber through the top vent valve
10) The sputtered sample is then removed and used for electroplating

2.4 Electrodepositon

Electroplating is often called as Electrodepositon. It is the process of depositing a metal layer on a surface by applying electric current. The metallic coating is obtained by giving a negative charge (cathode) to the anodisc (object to be electroplated) and dipping it into a solution with the salt of the metal layer that has to be deposited. As the metallic ions of the salt will be positively charged they will be attracted towards the object. As the ions reach the negatively charged object (anodisc) it provides electrons for positively charged ions to reduce to metallic form.

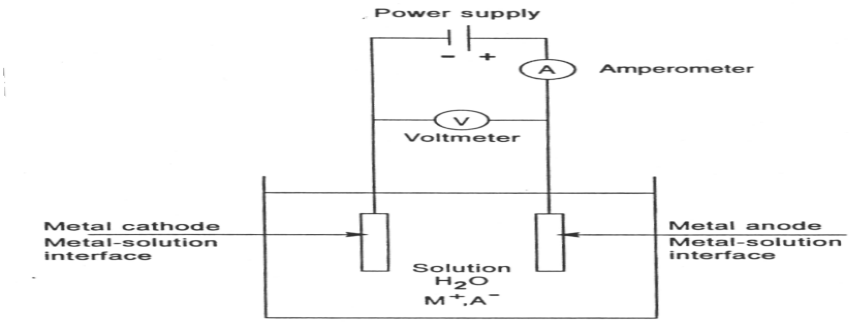

Fig 2.4 Electrolytic cell for electroplating metal ‘M’ from metal salt ‘MA’

Surface Pretreatment of by mechanical/chemical methods ensures good adhesion of the coating to the surface. Surface treatment and plating operations involve three basic steps

1) Surface cleaning or preparation - includes using of solvents, alkaline cleaners, acid cleaners, abrasive materials and/or water.
2) Surface modification - includes changing the surface attributes, such as application of metal layers and/or hardening.
3) Rinsing or other finishing operations to produce/obtain the final product.

Time is the primary factor which decides the thickness of the electroplated layer on the substrate. Typically layer thickness may vary from 0.1 to 30 microns[5]. The other factors include the geometric shape and contour of an object to be plated. In case of objects with sharp corners and features they will have thicker deposits on the outside corners and thinner deposits in recessed areas. It is because dc current flows more densely to sharp edges than to recessed ones. It is impossible to plate irregularly shaped items uniformly using electroplating but can be done with electroless plating.

To summarize the electroplating reactions, the reaction in aqueous medium at the cathode follows the equation with a corresponding anodic reaction.

M^{+n} + ne^{-} ==> M [2.7]

The deposition can be accomplished by two different paths:

1) Electrodepositon process – in this electrons are provided by an external power supply.
2) Electroless deposition process - in this a reducing agent in solution is the electron source.

Equation [2.7] is a deposition reaction of charged particles at the interface between a solid (metal) electrode and a liquid solution. Two types of charged particles that can cross the interface, they are metal ions M^{+n} and electrons e^{-}. The deposition reaction involves four types of issues. They are:

1) Structure and properties of the deposits.
2) Metal-solution interface as the locus of the deposition process.
3) Nucleation and growth process of the metal lattice.
4) Kinetics and mechanism of the deposition process.

Equation [2.7] is the reduction of a metal, which occurs during the plating process, for a single metallic ion. In order to reduce one mole of a given metal we need 'n' moles of electrons, i.e. the total cathodic charge used in the deposition 'Q' is the product of the number of gram moles of the metal deposited 'm', the number of electrons taking part in the reduction 'n', the electrical charge per electron 'Q_e', and Avogadro's number 'N_a' (the number of atoms in a mole),. Thus, the equation for the charge required to reduce 'm' mole of metal can be written as:

$$Q = m\ n\ N_a Q_e \qquad [2.8]$$

Substituting the Faraday constant in the above, the product of the last two terms in this by 'F'. Rearranging the above equation for number of moles of metal reduced by charge 'Q':

$$m = Q / (n\ F) \qquad [2.9]$$

The total charge used in the deposition can be written as the product of the current 'I' and the time of deposition 't'. In case the deposition current is held constant or the current is varied during the deposition:

$$Q = \int I\ dt \qquad [2.10]$$

Substituting and rewriting we get:

$$m = \frac{1}{nF \int I\, dt} \quad [2.11]$$

The weight of the deposit "w" is the product of atomic weight 'M_w' of the deposited metal and the number of moles of the metal reduced 'm'. Finally, to get the thickness of the layer deposited, we use the density of the metal 'D' (gram/cm^3):

$$D = w / V = w / (A\ T) \quad [2.12]$$

Where 'V' is the volume of the deposited metal in cm^3, 'A' is the area of the deposit in cm^2, and 'T' is its thickness in cm. Using Equations [2.11] and [2.12] we solve for thickness:

$$T = \frac{w}{AD} = \frac{M_w}{nFAD} \int I\, dt \quad [2.13]$$

Let us suppose, we take the current to be held constant during the deposition, the integral in Equation [2.10], can be written as 'I×t'.

2.5 Experimental section – Electrodeposition

1) The porous alumina (Anopore disc) with the gold sputtered layer is attached to a copper plate with a carbon tape. The sputtered side touches the Copper plate and the other side faces out.
2) In a beaker we fill the electrolyte ($CuSO_4 + H_2SO_4$) and the beaker is placed on a vibrational stirrer hot plate. I used the ceremag MIDI/IKA works. The temperature is raised to 60℃ and the stirrer is set to 2.5
3) A copper ring attached to a copper wire is used as the anode and the anodisc attached copper plate is the cathode.

4) Apply 1.5V DC supply for 40 min using a BK precision 1787B 0-72V/0-1.5A single o/p programmable DC power supply. The current increased from 0.01 to 0.04A. The Anodisc becomes red as the Copper is electroplated into it.
5) The copper plate is immersed into acetone for 10 min to remove the carbon tape and then the anodisc is inserted into 6M NaOH for 20 min and the porous alumina is dissolved and we are left with the nanowires.
6) The nanowires are rinsed well with de-ionized water so that they don't contain any NaOH. Then water is added to the nanowires and is placed into an ultrasonic vibrator (Elma Ultrasonic vibrator) for 15 minutes so that the nanowires will be well displaced in water

2.6 Summary of nanowire deposition

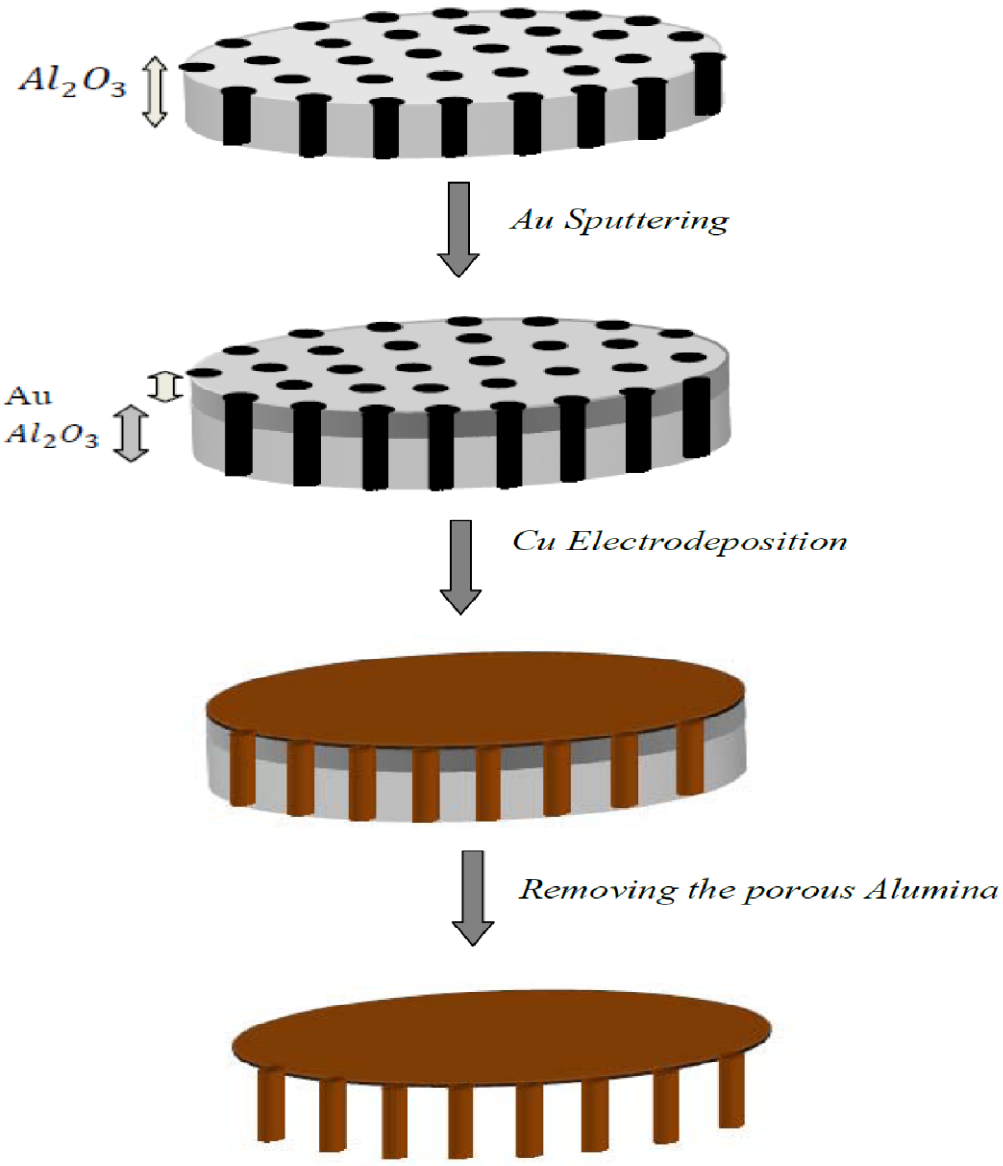

Fig 2.5 Summary of Copper nanowire deposition

2.7 Preparation of Gold Nanoparticles

1) Add 20 mL of 1.0 mM $HAuCl_4$ to a 50 mL beaker on a stirring hot plate (Ceremag MIDI/IKA works). Add a magnetic stir bar for stirring and bring the solution just to a boil.
2) As the solution starts boiling, add 2 mL of a 1% solution of trisodium citrate dihydrate, $Na_3C_6H_5O_7.2H_2O$. The gold colloidal solution starts forming gradually as the citrate reduces the gold (III). As the solution turns red the heater is turned off.

The formation of gold nanoparticles can be observed by a change in color since small nanoparticles of gold are red. The purpose of adding a layer of absorbed citrate anions on the surface of the nanoparticles is to keep the nanoparticles separated. For verification purposes the presence of the colloidal suspension can be detected by focusing a laser light on the particles and it gets reflected by the particles. If we switch to a smaller anion the particles approach more closely and another color change will observed[6]. The size of the gold nanoparticles obtained is 13nm (diameter).

2.8 4-Mercapto Pyridine molecule

The molecule we tested for SERS is 10^{-3}M 4-Mercapto Pyridine molecule. The molecular formula of 4 mercapto pyridine molecule is C_5H_5NS.

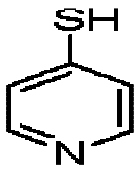

Fig 2.6 structure of 4 mercapto pyridine molecule

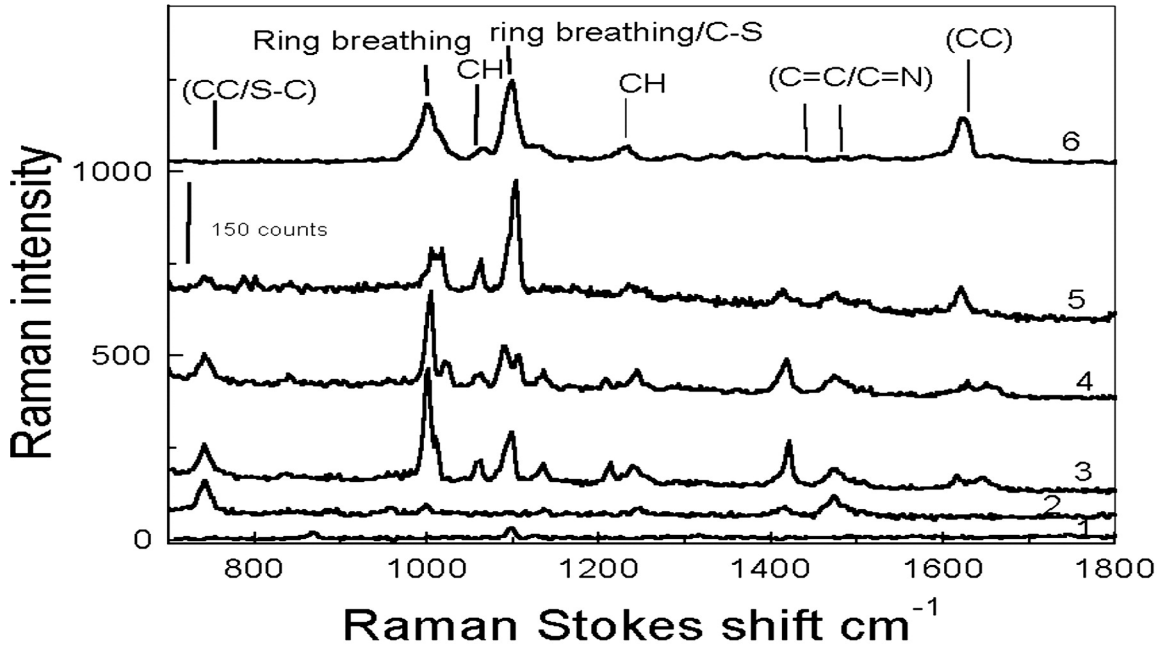

Fig 2.7 bulk and single molecule raman spectra of 4 mercapto pyridine molecule

Raman spectrum is a peak of the intensity of raman scattered light as a function of the frequency shift from the excitation wavelength (usually represented in wave numbers). This shift is known as Raman shift.

Fig 2.7 is Bulk and single-molecule Raman spectra of 4-mercaptopyridine on Tollens reaction silver surfaces. The CCD exposure time is 5 s for each spectrum and the excitation is 5 μW at 632.8 nm. Spectra 2–5 are representative Raman spectra of the same spot with time. Spectrum 6 is the bulk surface-enhanced Raman scattering spectrum of 4-mercaptopyridine for comparison. Spectrum 1 is the Raman spectrum of toluene on coverglass by using the same optical geometry and excitation power and a CCD integrated time of 15 s. The assignments of several prominent modes are listed on the spectra. In particular, they are C—H in plane wag ($843 cm^{-1}$), C—N double bond stretch ($1{,}200 cm^{-1}$)[7].

2.9 Atomic Layer Deposition (ALD)

ALD is a thin film deposition technique based on the sequential use of gas phase chemical process. The chemicals used are called precursors. The precursors react with the surface one at a time sequentially. After exposure of each precursor, the reaction chamber will be evacuated to remove the non reacted precursors and the gaseous reaction by products[8].

Repeated cycles of pulses of precursors lead to the growth of solid film. Layer thickness is given by the number of pulses multiplied by monolayer thickness. In theory, one monolayer per pulse is deposited, but in many cases a sub-monolayer growth is seen. In both cases, however, growth is self-limiting. Practical growth rates range around 1A° /cycle: for Al_2O_3 deposition, it is 1.1A° /cycle and for TiN, it is 0.2A° /cycle. When thickness/cycle numbers are translated into deposition rates, one has to take into account the flushing cycles between the pulses. Overall rates of a few nanometres per minute are typical for ALD, similar to LPCVD nitride or polysilicon, which are much higher temperature processes. ALD is a slow process, but there are many applications in which very thin films are needed, and step coverage requirements are strict: for example, diffusion barrier deposition into a high aspect ratio contact hole, or scaled down gate oxides. In both cases, a few nanometers are enough. ALD operating temperature is limited from below by two mechanisms low temperature leads to a low reaction rate (1), and precursor condensation on the surface leads to excessive deposition (2). The former leads to less than the monolayer deposition, and the latter to non-self-limiting deposition of unwanted composition. Upper operating temperature is also limited by two mechanisms: thermal decomposition of the precursors, which results in deposition in the

normal CVD fashion (3), and high re-evaporation rate, which leads to sub-monolayer growth per cycle (4). Under the right conditions, a uniform monolayer (or sub-monolayer) formation is observed[9].

ALD is a variant of CVD, but its deposition mechanism is different: in CVD, the deposition rate is strongly temperature dependent, but in ALD there is a (wide) process window in which the rate is independent of temperature. Uniformity of ALD is exceptionally good, with <1% uniformities reported for both within wafer and wafer to-wafer. ALD results in very conformal films. The nano laminate of aluminium and tantalum oxides covers the oxide step 100%, whereas the sputtered metal shows only ca. 50% step coverage. ALD is free of one of the main mechanisms of irreproducibility in CVD: homogeneous gas-phase reactions, which make, for instance, reaction $SiH_4 + O_2 \rightarrow SiO_2 + 2H_2$ prone to gas-phase SiO_2 particle generation. Because only one gas is introduced at a time, there cannot be gas-phase reactions between precursors.

2.9.1 ALD for depositing Aluminum oxide on the Anodisc

1) TMA (Trimethyl aluminum) reacts with the adsorbed hydroxyl groups producing methane as the byproduct.

$$Al(CH_3)_3 + :(PAA) - O - H \rightarrow :(PAA) - O - Al - (CH_3)_2 + CH_4 \quad [2.14]$$

2) TMA reacts with the adsorbed hydroxyl groups until the surface is passivated. TMA does not react with itself, limiting the reaction to one layer. This leads to the precise uniformity of ALD. The excess TMA is pumped away with the methane by product.
3) Water vapor is pulsed into the reaction chamber.

4) Water reacts with the dangling methyl groups on the new surface forming Al-O bridges and hydroxyl surface groups and methane is the reaction product.

$$2H_2O + :(PAA) - O - Al - (CH_3)_2 \rightarrow :(PAA) - O - Al - OH + 2CH_4 \quad [2.15]$$

5) Methane is pumped out. Excess water vapor does not react with hydroxyl surface groups.

6) Thus one TMA and one water vapor pulse form one cycle. The cycles are repeated basing on the thickness required[10].

CHAPTER 3

RAMAN SCATTERING AND SURFACE ENHANCED RAMAN SCATTERING

3.1 Raman Scattering

In order to develop complex materials with controlled properties we need to know the nature of chemical and physical processes at interfaces. To achieve this it is necessary to develop techniques for controlling and characterizing the molecular structure of interfaces in composite materials. Existing Surface analysis techniques such as UHV, XPS can detect a monolayer of most elements. They cannot provide direct information regarding molecular structures of adsorbed molecules on surfaces. They cannot be used to perform *in situ* analysis as they require conditions of high vacuum

Raman spectroscopy is an easy sampling technique, since bulk materials varying in shapes (films, powders, fibers, plates, pellets) may be studied without any modification. It works well in moist environments and can be used on samples having small areas. Thus Raman spectroscopy has its own advantages over other surface analysis techniques such as XPS, AES, HREELS, and IR.

3.1.1 Principle of Raman Scattering

When a photon of energy hv_o collides with a molecule two different types of light scattering can occur.

1) Rayleigh scattering
2) Raman scattering

Rayleigh scattering is an elastic collision between the incident photon and the molecule in which the photon neither loses nor gains energy. Raman scattering is an inelastic collision where the photon either gains energy from or loses energy to the molecule. The

energy of the scattered light is $h\ (v_0 + v_1)$ or $h\ (v_0 - v_1)$. The energy gained or lost hv_1 corresponds to the vibrational energy of the molecule. Thus the energy of the scattered light depends on the frequency of the incident light and the shift $hv_1$from the Rayleigh scattering line is a constant corresponding to the vibrational energy. I.e. the scattered light contains a spectrum of wavelengths in which the intensity peaks are shifted from the excitation wavelength by energy equivalent amounts corresponding to that for the excitation of the molecular vibration modes or crystal phonons. These vibrational spectra are highly specific for the material studied and can be used for unambiguous identification of substances. The Raman lines occurring at frequency $(v_0 - v_1)$ are called the Stokes lines and the lines occurring at frequency $(v_0 + v_1)$ as anti-Stokes lines. The stokes lines are of higher intensity than anti stokes lines due to the Boltzmann distribution – i.e., due to higher population of molecules in the ground state than in the excited state. Because of this feature of stoke lines we use them in the study of Raman scattering.

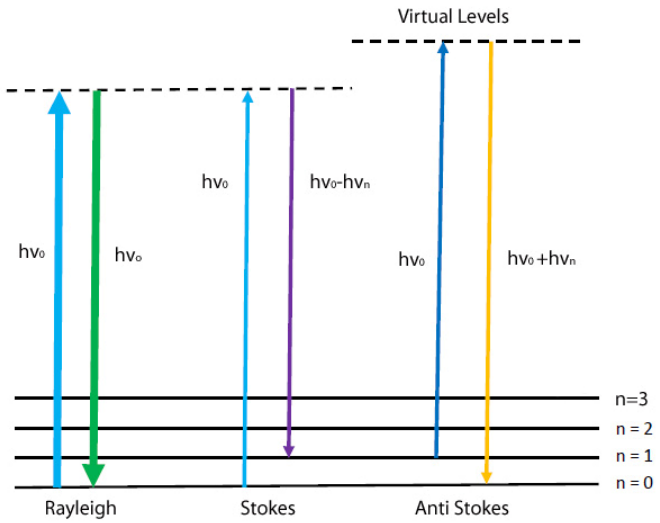

Fig 3.1 Idealized model of Rayleigh, Stokes, Anti-Stokes scattering

3.1.2 Instrumentation

In 1928 C.V. Raman observed the scattering effect, using sunlight and complementary filters[11]. Later mercury vapor lamps were used for illumination of samples. Current Raman spectrometers use lasers as monochromatic light sources and the type of laser depends on the wavelength, sensitivity and spectral resolution required. Sample optics are used to focus the laser on to the sample and collect the Raman scattered light. In the wide spread backscattering or 180° arrangement a single objective serves for both, focusing the laser and collecting the scattered light.

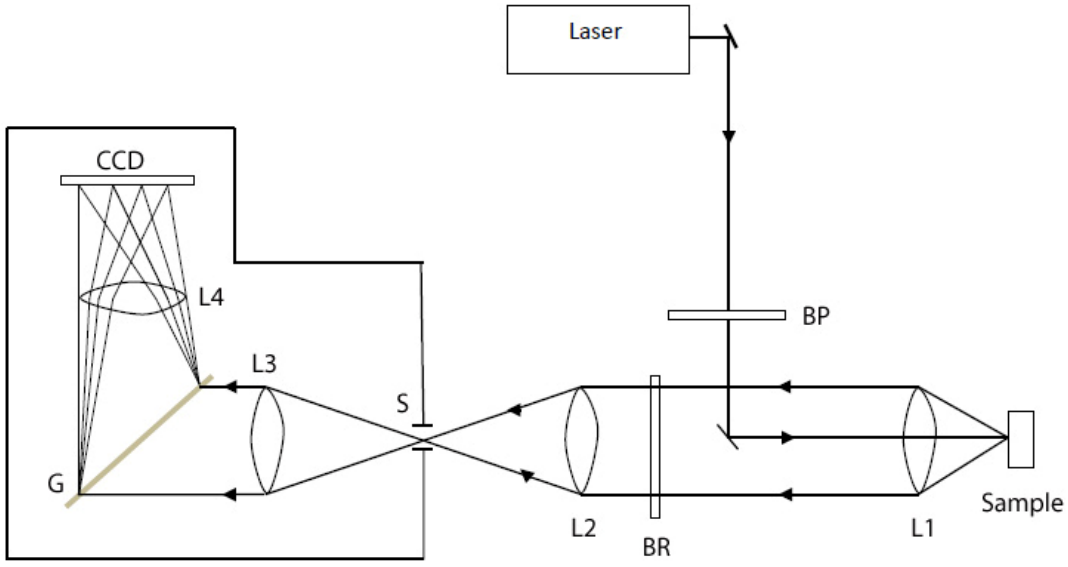

Fig 3.2 Example of sensitive Raman equipment

Elastically scattered light must be removed in front of the spectrometer as it has more intensity than the Raman scattered light and would produce stray radiation at the

detector and holographic notch filters are used for this purpose. Spectral analysis of the Raman scattered light is done by dispersive or Fourier Transform (FT) spectrometers.

Different accessories are available for Raman spectroscopy. Confocal microscopes afford lateral resolution of approximately $1\mu m$ and depth resolution down to approximately $2\mu m$[12]. The depth resolution is especially important for surface and interface spectroscopy, because it helps to eliminate Raman intensities from the bulk phases. Fiber optics can be used to guide the exciting laser light to the sample and the scattered light to the spectrometer. This makes changing the samples easier and eliminates the hazards of freely propagating laser light. Special sample cells have been constructed for measurement at high or low temperatures and at high pressures, and for laser multi-pass through gaseous samples.

3.1.3 Spectral Information

For large molecules, Raman spectra contains numerous bands which cannot always be assigned to particular vibrational modes. However the large number of bands when measured with appropriate spectral resolution enables unambiguous identification of substances by comparing the spectra. Vibrations of weakly polar and even symmetrically bonded atoms usually result in intense Raman bands as Raman activity is related to changes in molecular polarizability during vibration. Structural isomers usually have different spectra and can be easily distinguished. Polarization effects are another feature of Raman spectroscopy that improves the assignment of bands and enables the determination of molecular orientation. Analysis of the polarized and non-polarized bands of isotropic phases enables determination of the symmetry of respective vibrations. For aligned molecules in crystals or at surfaces it is possible to measure the dependence

of upto six independent Raman spectra on the polarization and direction of propagation of incident and scattered light relative to the molecular or crystal axes.

The intensity of the scattered radiation depends not only on the polarizability and concentration of the analyte molecules, but also on the optical properties of the sample and adjustment of the instrument. Absolute Raman intensities are therefore not an accurate measure of concentration. These intensities are useful for quantification under well defined experimental conditions and for well characterized samples.

One limitation of Raman Spectroscopy for studying thin organic films adsorbed onto metal surfaces is that the low intensity of the Raman scattering must be detected in the presence of a large background. The problem of low Raman cross section has been dealt with SERS (Surface enhanced Raman scattering).

3.2 Background of Surface Enhanced Raman Scattering

Surface Enhanced Raman Scattering (SERS), is a surface sensitive technique that results in the enhancement of Raman scattering signals by molecules adsorbed on nanometer sized rough metal surfaces. When compared with the Raman signal the enhancement is $10^{14} - 10^{15}$ times higher, thus making it sensitive enough to detect single molecules[13]. The main problems encountered with SERS are fluctuations in signals, lack of reproducibility, and lack of understanding of the origin and conditions for SERS, lack of control over the magnitudes and spatial location of hotspots responsible for enhancement.

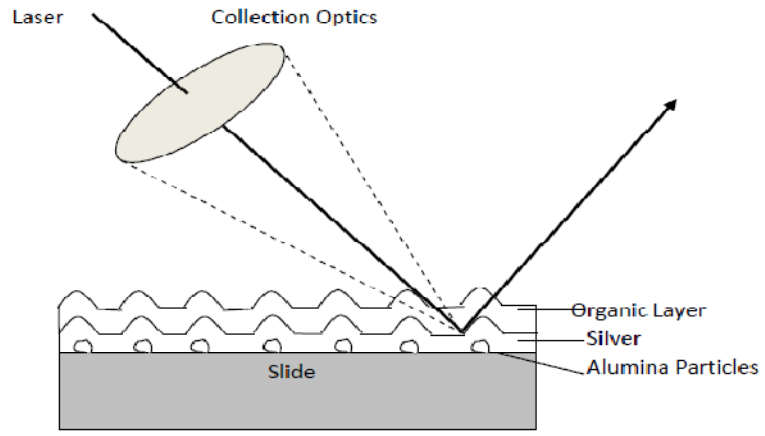

Fig 3.3 SERS active substrate and the measurement arrangement.

As in Fig 3.3 Alumina nanoparticles deposited on the glass slide provide the required roughness. Silver layer evaporated on to the nanoparticles provides the enhancement. Organic molecules adsorbed on the Silver surface can be detected by irradiation with a laser and collecting the Raman scattered light.

SERS is more complex compared to Raman scattering. When we consider the Raman vibrational spectrum of a molecule in gas phase, the basic components involved in this are just the molecule and the incident radiation. In contrast, in SERS, the basic components involved are a molecule, a metal nanostructure and electromagnetic radiation. This difference introduces greater complexity to the SERS measurements. The important challenges to the interpretation of SERS spectra are:

1) The molecule interacts with a metal nanostructure. The adsorption on solid surfaces can be divided according to the strength of bonding between the particle and the substrate into two categories, physisorption and chemisorption. Physisorption refers to the weak interactions arising from van der Waals forces,

with adsorption energies well below those of normal chemical bonds. Physical adsorption may alter the surface structure of molecular solids but not that of metals. When the adsorption energy is large enough and comparable to chemical bond energies, chemisorption is used.

2) Incident photons can induce substrate excitations such as electron hole pairs, surface plasmons or surface phonons that may be involved in the enhancement of photo-induced processes. The most important one is that absorption of light by nanostructures can create strong local electric fields at the location of the adsorbed species. This enhanced local field will strongly affect the optical properties of the adsorbate and is the main factor for the SERS effect.
3) Interaction of incident light with adsorbed molecules may lead to photo dissociation, photoreactions or photo desorption. All these processes can leave their own effects in SERS spectra.
4) Interaction of light with metallic nanostructure depends on the value of complex dielectric function at the excitation wavelength and this will determine the enhancement observed at a particular frequency of excitation. Particle absorption and scattering depend on the shape and size of the metal nanostructure, SERS intensities are also influenced by these. In addition, the excitations in nanostructures are strongly influenced by the dielectric constant of the medium.
5) The dynamics of the interaction of light with the adsorbate leads to a pattern of Raman intensities determined by the selection rules. A distinction between the selection rules for vibrational transitions of a molecule in the gas phase and the surface selection rules for a fixed spatially oriented molecule at the surface of an

enhancing nanostructure. Surface selection rule encompass the symmetry properties of the dipole transitions and the modification of the intensities due to the components of local electric field vector at the surface. They apply to molecules anchored on nanostructures where Raman and infrared intensities are further modulated by the spatial orientation of the local electric field interacting with the polarizability derivative tensor. Since the adsorbed molecule generally belongs to a different symmetry point group than that of the parent molecule, the corresponding allowed modes and their polarization are also different.

6) SERS is obtained by excitation with visible or near infrared light. The presence of metal nanostructures may permit new excitations in the molecule-nanostructure complex, such as charge transfer transitions from the Fermi to LUMO level of the molecule. Since the excitation is in resonance with the electronic transition of the adsorbed metal complex, the inelastic scattering is due to resonance Raman scattering (SERRS).
7) Small amounts of impurities may sometimes be responsible for the sudden signals that further complicate the interpretation of the observed SERS spectra.

In 1974 Martin Fleischman observed SERS from pyridine adsorbed on electrochemically roughened silver electrode and their analysis of the large signal was due to increase in effective surface area due to roughening of silver electrode, which is due to number of molecules scattering on the surface[14], and they did not recognize the major enhancement. Three years later two groups noted that the concentration of scattering species alone cannot be responsible for the enhanced signal and each proposed

a separate mechanism for the enhancement. These formed the underlying principles for the SERS effect. Jeanmaire and Van Duyne proposed a charge-transfer effect[15], while Albrecht and Creighton proposed an electromagnetic effect[16]. There is a disagreement over the absolute and relative enhancement factors among the Electromagnetic effect and the charge transfer effect even today. It is because both Electromagnetic and Charge transfer methods are critical roughness based models. These two mechanisms arise because the intensity of Raman scattering is directly proportional to the square of the induced dipole moment, μ_{ind}, which, in turn, is the product of the Raman polarizability, α, and the magnitude of the incident electromagnetic field, E.

When optimizing for the SERS activity, the surfaces are very rough, consisting of various roughness components ranging from atomic to sub micron size. Therefore it is difficult to distinguish the contribution from the EM and CT models[17].

3.2.1 Electromagnetic theory

The Raman signal intensity can be enhanced greatly on certain surfaces because of excitation of surface plasmons, which enhance the electric field near the surface. When the incident light strikes the bulk of the metal surface, localized surface plasmons are excited. The field enhancement is greatest when the plasmon frequency,ω_p, is in resonance with the radiation. In order for scattering to occur, the plasmon oscillations must be perpendicular to the surface; if they are in-plane with the surface, no scattering will occur. When free electrons scatter, the component of the scattering vector parallel to the surface is responsible for the excitation of localized surface plasmons. This requirement is the reason for using rough surfaces or nanoparticle arrangements in SERS

experiments as they can provide an area where localized collective oscillations take place[18].

When light is incident on a surface it can excite different phenomena and this complexity can be made negligible by surfaces much smaller than the wavelength of the light, in such cases only dipolar contributions will be recognized by the system. The dipolar term contributes to the plasmon oscillations, which leads to the enhancement. SERS effect is so pronounced, because the field enhancement occurs twice. Initially, the field enhancement magnifies the intensity of incident light which will excite the Raman modes of the molecule being studied, therefore increasing the signal of the Raman scattering. The Raman signal is then further magnified by the surface by the same mechanism as the incident light was, resulting in a greater increase in the total output signal of the experiment. The enhancement factor E at each molecule is given by

$$\mathrm{E} = |\mathrm{E}(\omega)|^2 |\mathrm{E}(\omega')|^2 \qquad [3.1]$$

Where $E(\omega)$ is the local electric field enhancement factor at the incident frequency ω and $E(\omega')$ is the corresponding factor at the stoke shifted frequency ω'. In conventional SERS, E is averaged over the surface area of the particles where molecules can adsorb to generate the observed enhancement factor <E>, while in single-molecule SERS (SMSERS) it is the maximum enhancement E_{max} that is of interest.

The enhancement varies with frequency. For frequencies in which the Raman signal is only slightly shifted from the incident light, both the incident laser light and the Raman signal can be near resonance with the plasmon frequency, leading to the E^4 enhancement. If the frequency shift is large, the incident light and the Raman signal

cannot both be in resonance with ω_p, thus the enhancement at both stages cannot be maximal[19].

Plasmon resonance frequency decides the surface metal that needs to be used. Visible and near-infrared radiation (NIR) is used to excite Raman modes. As the plasmon resonance frequencies of gold, silver, copper fall within these wavelength ranges, these metals are mostly used so that they provide maximal enhancement for visible and NIR light[20]. Platinum and palladium nanostructures also display plasmon resonance within visible and NIR frequencies[21].

3.2.2 Chemical Enhancement

Chemical enhancement corresponds to any modification of the Raman polarizability tensor upon adsorption of the molecule onto the metal surface. Such a modification, in some cases can lead to destroying the enhancement. The required chemical enhancement occurs when the modified polarizability is more resonant with the excitation than with the effect of charge transfer mechanism in the metal adsorbate complex. As a result of the resonant condition the Raman intensity increases. Chemical enhancement does not require chemically bound molecules but in order to account through charge transfer we need a covalent bond. The chemical enhancement is multiplicative and occurs along with electromagnetic enhancement.

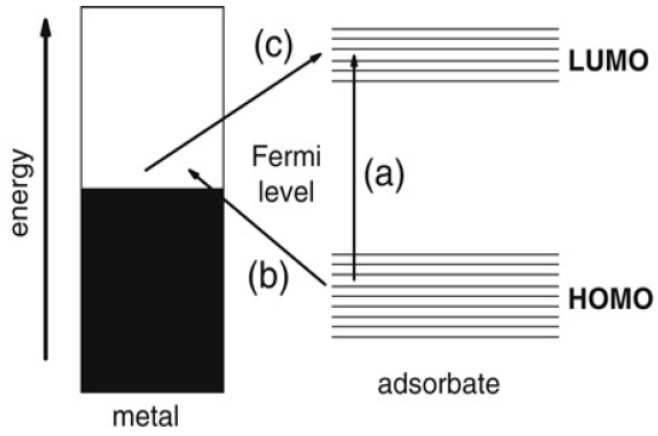

Fig 3.4 schematic representation of charge transfer effect

Charge transfer mechanism is the most studied mechanism for the chemical enhancement. The schematic representation of the effect can be seen in the fig 3.4. The various scenarios possible for the chemical enhancement are[22]:

Type I occurs when the adsorbate does not bind covalently to the metal. In this case, the presence of the metal acts only as a perturbation to the electronic structure of the analyte causing a mild change in its electronic distribution. This leads to a corresponding change of polarizability and, as a result changes the Raman efficiency of the mode.

Type II is like the one in fig 3.4, it involves the presence of a surface complex either by direct (covalent) binding to the metal, or by indirect binding with the assistance of an electrolyte ion (typically chloride). This may produce a substantial change in the intrinsic polarizability of the molecule. As the magnitude of the polarizability depends explicitly on the available optical transitions, the new indirect transitions provided by the overlap of molecular orbitals provide a channel for the polarizability to be modified. It is possible also that the surface complex creates a new electronic state (similarly to the gap

states created at the surfaces of semiconductors) that is explicitly in resonance or close to resonance with the laser, hence providing a contribution to the enhancement of a resonant-Raman type.

Type III is a complex version of type II which involves the process of photo-driven charge transfer between the analyte and the metal. This situation can occur when the difference between the Fermi level E_F of the metal and the HOMO or LUMO energies is matched by the laser. A photo-driven charge-transfer mechanism between the HOMO and unoccupied states above the Fermi level (or between the LUMO and occupied states slightly below E_F) can be triggered. This mechanism was uncovered through experiments in electrochemical cells where it is possible to change the difference in energy between the adsorbed analyte and the metal through an external potential. The maximum SERS intensity is observed at different potentials for different incident laser energies. The interpretation of this is that different tuning conditions are needed depending on the laser energy being used, and this tuning is provided by the external potential.

These experiments can serve as proof, that charge transfer mechanisms between the molecules and the substrates are real and can play a non-negligible role in the magnitude of the SERS enhancement.

3.2.3 Surfaces

SERS is a surface sensitive technique. The first experiments were performed on electrochemically roughened silver. Now surfaces are often prepared using a distribution of metal nanoparticles on the surface[23].

The signal enhancement depends on the shape and size of the metal nanoparticles as these factors influence the ratio of absorption and scattering events. There is an ideal size for these particles—any small particles will not have the same impact on the Raman intensity—and there exists an ideal surface thickness for each experiment. For the SERS to occur metal particles or metal features responsible for its operation should be small with respect to the wavelength of the exciting light i.e. the SERS active systems should possess structure in the range of 5-100nm range. Likewise, the dimensions of the active structure cannot be smaller than the molecule and the upper bound is determined by the excitation wavelength. If the particles are too large they allow the excitation of multipoles which are nonradiative. Only the dipole transition leads to Raman scattering and the higher-order transitions will decrease the overall efficiency of the enhancement. If the particles too small, they lose their electrical conductance and cannot enhance the field. Also when the particle size approaches a few atoms, the definition of a plasmon does not hold, as there must be a large collection of electrons to oscillate together[24].

SERS enhancement of silver is more than gold followed by copper. The reason can be explained with a simple rudimentary model[31]. The polarizability of a small metal sphere with dielectric function $\varepsilon(\lambda)$ and radius *R* surrounded by a vacuum is given by

$$\alpha = R^3 \frac{\varepsilon - 1}{\varepsilon + 2} \qquad [3.2]$$

Combining this expression with the expression for dielectric function of Drude metal slightly modified by interband transitions is given by

$$\varepsilon = \varepsilon_b + 1 - \frac{\omega_p^2}{\omega^2 + i\omega\gamma} \qquad [3.3]$$

Where ε_b is the contribution of interband transitions to the dielectric function

ω_p is the metal plasmon resonance

γ is the electron scattering rate, inversely proportional to the metal's DC conductivity

Combining the above two equations yields

$$\alpha = \frac{R^3\left(\varepsilon_b\omega^2-\omega_p^2\right)+i\omega\gamma\varepsilon_b}{\left((\varepsilon_b+3)\omega^2-\omega_p^2\right)+i\omega\gamma(\varepsilon_b+3)} \quad [3.4]$$

Hence, when is γ large, either because of the inherent poor conductivity of the metal or due to the fact that the metal nano features are so small that electronic scattering at the particles surfaces become the dominant electron-scattering process, the quality of the resonance is reduced, and with it the SERS enhancement. And for metals with high ε_b , the width of the resonance is increased and hence the SERS enhancement decreases. Most transition metals are poor SERS-enhancing systems because, for them, the two effects combine to reduce their SERS enhancement ability, i.e. their conductivity is low (γ is large) and the interband contribution to the dielectric function is great (ε_b is large).

3.2.4 Selection Rules

SERS provides the same information as Raman spectroscopy but with a greatly enhanced signal. The spectra of most SERS experiments are similar to the non-surface enhanced spectra, often there are differences in the number of modes present. Additional modes can be present in the SERS spectrum, while other modes can disappear in comparison to the Raman spectra.

The modes observed in any spectroscopic experiment are directly dependent on the symmetry of the molecules and are usually summarized by selection rules. When molecules are adsorbed to a surface, the symmetry of the system can change, and even a slight modification of the symmetry of the molecule can lead to differences in mode selection[25].

One common way in which selection rules are modified arises from the fact that many molecules that have a center of symmetry lose that feature when adsorbed to a surface. When this happens there is no need of mutual exclusion, which dictates that modes can only be either Raman or Infrared active. Thus, modes that would normally appear only in the infrared spectrum can appear in the SERS spectrum.

The symmetry of a molecule can be changed in different ways depending on the orientation in which the molecule is attached to the substrate. In some experiments, it is possible to determine the orientation of adsorption to the substrate from the SERS spectrum, as different modes will be present depending on the way in which the symmetry is modified[26].

3.3 Scanning electron microscope (SEM)

The first SEM was developed in 1942 and the first commercial one was out in 1965. SEM can produce images of greater clarity[27], 3-D quality and require less sample preparation. Hence SEM is more popular than TEM (Transmission electron microscopy) even though it can produce images of greater magnification. The SEM can produce images in the range of 10 to 100,000 times their normal size. It has a rather large depth of field, i.e. more of the image being magnified is in focus. The SEM produces a sharp, 3D view of a spectrum and is very helpful in analyzing its shape and structure.

In a SEM an electron gun emits a beam of electrons, which passes through a condenser lens and is refined into a thin stream. From there the objective lens focuses the electron beam onto the specimen. The objective lens contains a set of coils which are energised with varying voltages. The coils create an electromagnetic field that exerts a

force upon the electrons in the electron beam, which in turn redirects the electrons to scan the specimen in a controlled pattern called a raster. The electromagnetic field of coils also causes a spot of light on a cathode ray tube to move along at the same rate as the scanning electron beam. When the electrons from the beam hit the specimen, a series of interactions deflect secondary particles to a detector, which then converts the signal to voltage and amplifies it. This voltage is then applied to a cathode ray tube and converted to an image. The intensity of the image is determined by the number of secondary particles that hit the cathode ray tube, which is dependent upon the angle the electrons bounce off the specimen.

When an electron from the beam encounters a nucleus in the specimen, the resultant attraction produces a deflection in the electrons path. A few of these electrons will be completely backscattered re-emerging from the surface of the sample. Since the scattering angle is strongly dependent on the atomic number of the nucleus involved, the primary electrons arriving at a given detector position can be used to yield images containing information on both topology and atomic composition. Some of the beam's electrons can also interact with the electrons in the sample. The amount of energy given to these secondary electrons as a result of the interactions is small, and so they have a very limited range of few nanometers and often do not escape. The electrons that are a very short distance from the surface are able to escape and are observed by the detector. The images from these secondary particles contain a lot of detailed information. This implies that using secondary particles as imaging data boosts higher resolution topographical images.

One drawback of SEM is that it cannot be used to analyze specimens that give off any type of vapor. This vapor would interact with electrons. This problem can be overcome by using cryogenic SEM, where the specimen is frozen and coated with gold so that the vacuum tube can remain relatively free of vapor. In the recent years SEM has been made with a controlled vacuum chamber, where the top of the chamber is a vacuum and the very bottom of the chamber is kept at near vacuum. This allows the natural expulsion of particles from wet samples, so the microscope can analyze crystallizing and drying.

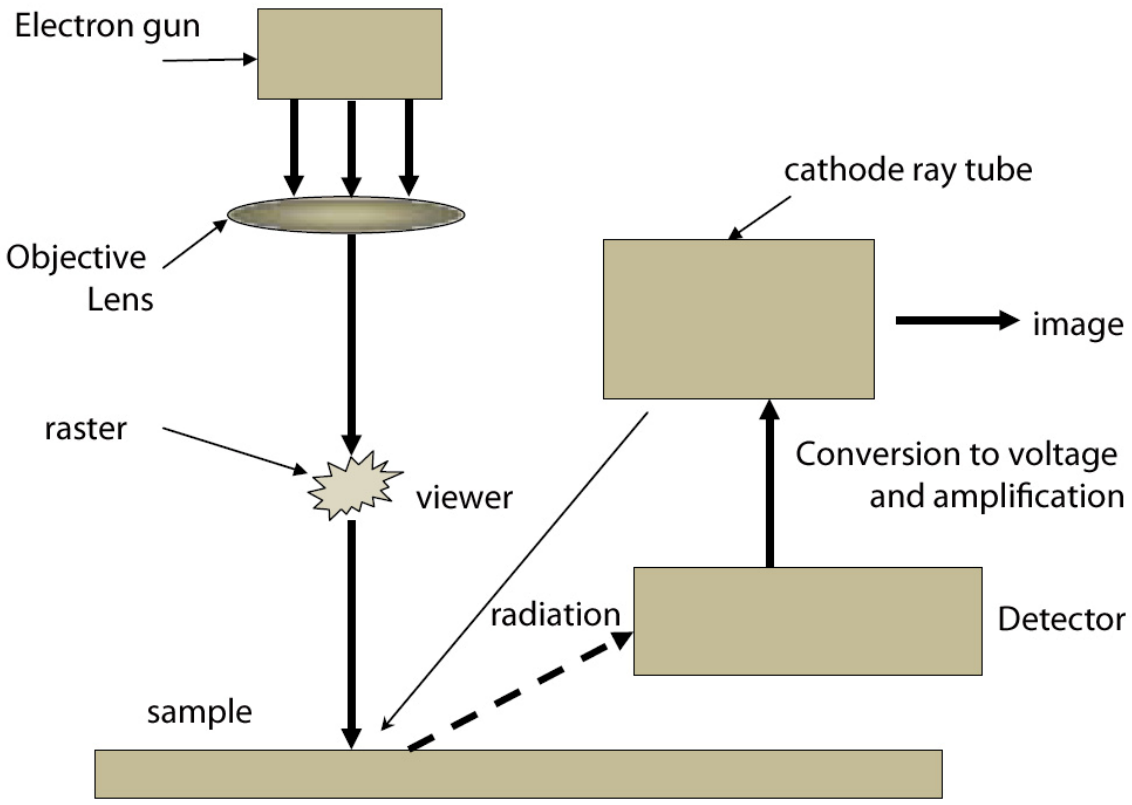

Fig 3.5 Simplified view of a scanning electron microscope

CHAPTER 4

APPLICATIONS OF SERS

Many advances have been made in chemical and bio sensors based on surface enhanced Raman scattering (SERS). In order to detect minute amounts of a compound in a real-life sample, sensors must be able to differentiate compounds having different molecular sizes and also identify specific substituents and/or derivative chemical groups attached to the basic structure.

The SERS substrate is inserted directly into the cell and the SERS spectrum is recorded. For in the place measurements, the substrates are mounted on a fiber optic probe and inserted into liquid samples for spectral recording.

The SERS substrates were also used in chemical vapor sensors. Following exposure to the analyte vapor, the SERS substrate was removed from the dosimeter and inserted directly into the Raman spectrometer. The SERS spectrum was then recorded.

SERS data is collected in two ways. The most common technique uses the front side excitation/collection geometry. In this geometry, the excitation beam is focused onto the front (metal) side of the SERS substrate and scattered radiation was also collected from the front side at 90 ° with respect to the excitation beam. An optical fiber-based auxiliary optical setup was also used for some measurements. With this remote setup, the excitation fiber is placed at the back (glass) side of the SERS substrate, while the collection fiber is placed at the front (metal) side of the substrate at an angle of 180° with respect to the excitation fiber.

4.1 Remote Fiber Optic SERS monitors and nanosensors

Metallic nano structures on solid substrates can directly be integrated with sensors unlike the other techniques. Development of SERS active substrates for direct measurement in liquid samples is the most critical and needed. Remote fiber optic monitors have two configurations.

4.1.1 Dual fiber system

One fiber is used for transmitting the laser excitation, the second fiber for transmitting the Raman signal[28].The SERS probe is prepared with a microscope slide (1mm thick) so that the excitation probe can be positioned head on or one on each side. The terminus end of the collection fiber was positioned next to the entrance slit of a spectrometer. Since the f/number of the fiber and that of the spectrometer were different, it was necessary to focus the input radiation from the collection fiber with lenses. An f/1 lens is used to collect and collimate the output beam from the collection fiber. A second lens with an f/number matching that of the spectrometer (f/7) is then used to focus the collected

SERS signal into the slit of the spectrometer equipped with a red-enhanced intensified charge-coupled device (ICCD). With excitation and collection fibers of up to 20 m length, this remote SERS sensor can detect various analytes in millisecond time periods.

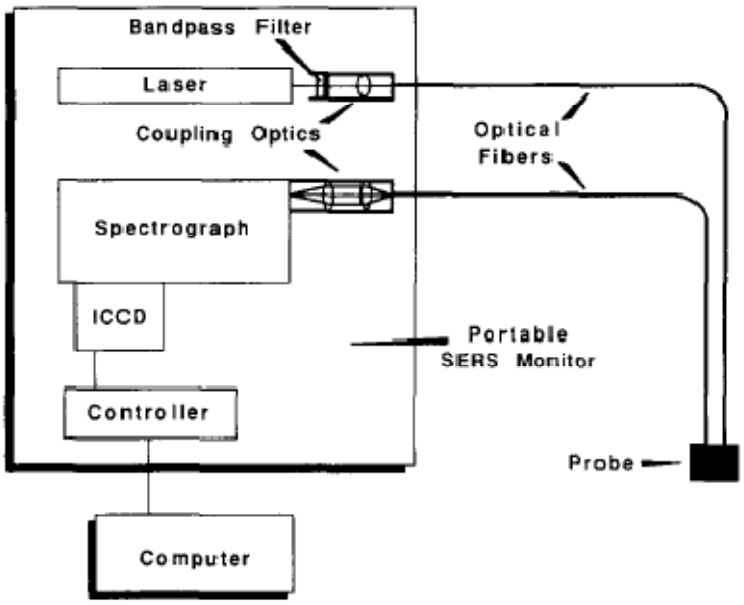

Fig 4.1 Schematic diagram of Dual fiber based SERS probe system

4.1.2 Single Fiber System

Helium-Neon laser is used to provide the 632.8nm radiation. It is spectrally purified by a bandpass filter. A holographic beam splitter is used to direct the entire beam into an objective lens, the objective lens focuses the beam on to the SERS sensor fiber for sample excitation. The signal returning from the SERS-active tip was collected and collimated by the same objective lens. The expanded signal beam is nearly 100% transmitted through the holographic beam splitter to a silica lens which focused the signal beam onto a second 600μm optical fiber. A Raman Holographic notch filter (Physical Optics Corporation) is also used to reject any unwanted reflected or Rayleigh-scattered radiation from the expanded signal beam prior to focusing onto the second optical fiber, which carried the signal to the spectrograph for detection. A two-lens system is used to provide an efficient coupling between the optical fiber and the spectrograph. The

spectrograph is a 320-mm polychromator (ISA, Model HR-320) equipped with a single 600-g /mm holographic grating and a red-enhanced intensified charge coupled device (RE-ICCD). All measurements are performed with an entrance slit width of 30 μm, resulting in a resolution of approximately 3.3cm^{-1} at 675 nm. The RE-ICCD (Princeton Instruments,

Model RE/ ICCD 576S) was thermoelectrically cooled to -34°C.

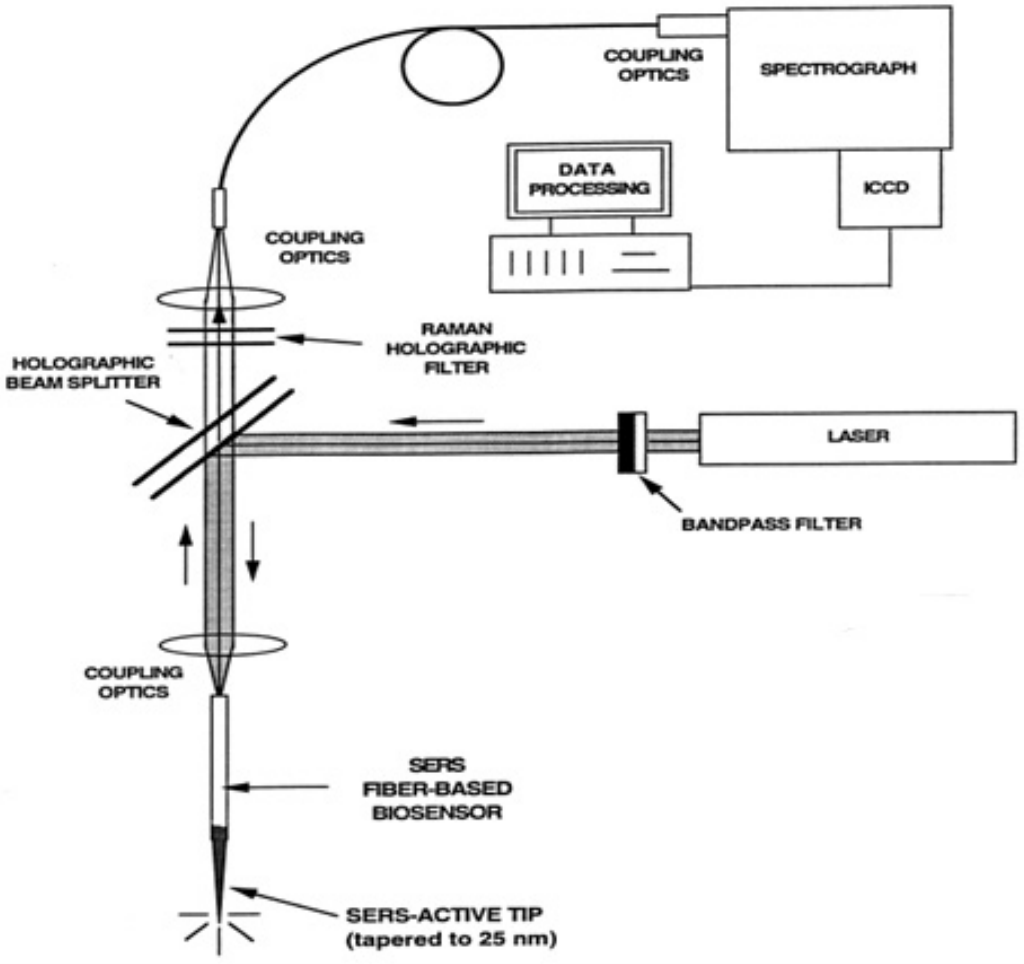

Fig 4.2 Schematic diagram of Single Fiber based SERS Probe System

The small diameter of the optical fiber allows direct entry into smaller sample environments, minimizing sample handling

4.2 SERS Vapor Dosimeter

The device employs SERS for direct measurement of the amount of chemical vapor collected on the dosimeter. The working involves three steps

1) Sample collection via a diffusion controlled process
2) Adsorption of analyte molecule on the substrate
3) Direct detection using SERS technique

The SERS dosimeter is a self-contained, badge-size passive monitor. The dosimeter consists of a badge-size sample holder, a SERS-active substrate, and an interchangeable diffusion tube. The screen device serves to prevent air turbulence from affecting the diffusion process within the dosimeter. Vapor collection of the dosimeter is based on molecular diffusion. A solid sorbent material is placed at the closed end (x=0) of the tube while the open inlet of the tube (x=L) is exposed to the outside concentration, C_o of analyte vapor molecules. The heart of the SERS dosimeter is the sample collection material that consists of SERS-active substrate.

The sorbent material maintains the concentration of the analyte compounds at the collection surface at zero or near zero concentration, C_s, while the air outside the dosimeter is at ambient concentration. A concentration gradient is therefore maintained, which serves as a driving force inducing the diffusion of the analyte molecules from the outside of the dosimeter onto the SERS-active surface.

The molecules that diffuse through the tube are collected and adsorbed onto a SERS-active substrate that also serves as a direct sample medium for Raman detection.

The unique feature of this dosimeter is the dual purpose of the SERS substrate that serves as both a sample collector/ sorbent and a Raman signal enhancer. The procedures developed for analyzing the dosimeters are very simple since the dosimeters can be inserted into detector for direct reading of the integrated exposure immediately after exposure[29]. The passive SERS monitor described here could provide a simple and low-cost approach for monitoring chemical vapors and obtain much needed information on human exposure to potentially hazardous pollutants.

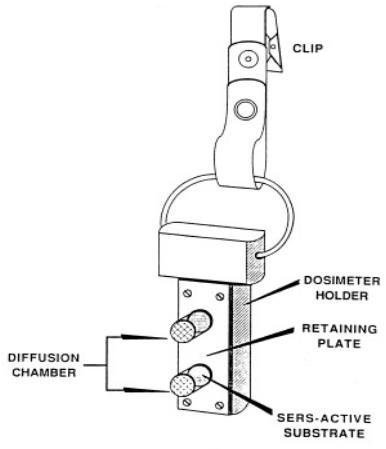

Fig 4.3 Schematic design of SERS dosimeter

4.3 Single molecule detection using SERS

Under appropriate conditions SERS enhancements of 10^{14} have been obtained. This degree of enhancements is enough for single molecule detection. This has brought hope for ultrasensitive analytical strategies and bioassays based on SERS. The essential step for the successful implementation of single molecule SERS lies in constructing small, properly organized nanoparticle clusters with interstices of the proper dimensions

and chemical affinity in which the molecular analyte can reside and benefit from inordinate optical field enhancement localized at that spot.

Electromagnetic calculations indicate that the enhancements possible with such structures will be seldom greater than 10^{11}, whereas the single molecule SERS experiments indicate that the enhancements are as high as 10^{14}. The extra enhancement is likely due to chemical enhancement, which involves resonant processes located mostly on the adsorbed molecule or due to the adsorption process. This is the reason why not all adsorbed molecules seem capable of producing single molecule SERS.

Even without these chemical processes, the electromagnetic enhancement with properly designed metal nanostructures can lead to highly sensitive analytical techniques with sensitivities down to a few thousand molecules.

4.4 SERS for Protein detection

The ability of proteins to bind other molecules specifically and tightly gives them diverse functions. Early studies of proteins focused on SERS spectra of individual proteins and the successful design of nanoparticle probes led to the progress of SERS based immune assays. Usually the SERS active substrates are prepared first, then analytes are added for further SERS detection. A different approach in which the substrate is mediated by the target proteins used for detection enhanced the results[30].

The SERS based methods for protein detection are divided into two types based on the target objectives.

1) Label free strategy
2) Raman dye labeled

The label free strategy involves getting the proteins on the SERS substrates and getting the SERS spectrum while in the dye labeled strategy proteins are indirectly detected by SERS of Raman dyes that are linked to the Raman probes.

CHAPTER 5

FACTORS INFLUENCING SERS

5.1 Effect of Electromagnetic enhancement in absence of adsorbed molecule

It is universally observed that the intensity of the enhanced background increases when molecules are adsorbed on the SERS active system. This rises the idea that the SERS mechanism is turned on only in the presence of adsorbed molecules.

The question raised above is not true. First, although the intensity of the enhanced background increases upon adsorption, it is present even in the absence of adsorbate and even in films produced under high vacuum in which the films can be regarded as free of adsorbate. Hence the molecule may simply be modifying the selection rules leading to the electronic process responsible for the enhanced background.

A more convincing demonstration of the inherent electromagnetic enhancement in the absence of adsorbate was reported by Stuckless and Moskovits[31] and expanded by Shalaev[32]. Photoemission was measured from smooth and rough silver surfaces produced under ultrahigh vacuum. The results demonstrate dramatically the effect of electromagnetic enhancement. When the silver surfaces were excited with 4.54 eV photons, which are not resonant with the plasmon, both rough and smooth surfaces produced similar photoemission fluxes within a factor of 2 that can be accounted for easily in terms of the increased surface area of the rough surface. Moreover, the fact that this enhancement was not seen when the same SERS-active surfaces were illuminated with photons that were well above resonance with the localized surface plasmon suggests that it is unlikely that some mechanism other than electromagnetic enhancement is responsible for the dramatically increased photoelectron yield observed for rough silver.

5.2 Isolated nanoparticles vs aggregate nanoparticles for SERS

Most of the SERS active systems are assemblies of interacting particles like nanoparticle aggregates, rough metal surfaces, and island films. Isolated particles are not preferred for SERS. In case of assemblies of isolated particles the interaction is through space electromagnetic coupling, which will be dominated by dipolar coupling and includes multi polar coupling in case of closely spaced particles.

SERS intensity can be greatly enhanced when two or more nanoparticles are brought close together. It was reported by Xu and Kall[33] when two nanoparticles are brought close together the optical field strength in the interstice between the two particles can be increased to obtain SERS enhancements of 10^{11} for molecules residing at that spot. The conditions used in obtaining the enhancement were the distance between the nanoparticles is < 5 nm, light of appropriate wavelength is used and exciting electric field vector is polarized along the interparticle axis. This giant enhancement, which exceeds that at isolated metal particles by about six orders of magnitude, falls off rapidly as the interparticle gap increases. For light polarized across the interparticle axis, the enhancement is almost negligibly different from its value at a single, isolated particle.

All aspects of this effect can be explained in terms of some very simple physics. Referring to Fig. 5.1, a molecule (indicated by a small circle in the figure) located

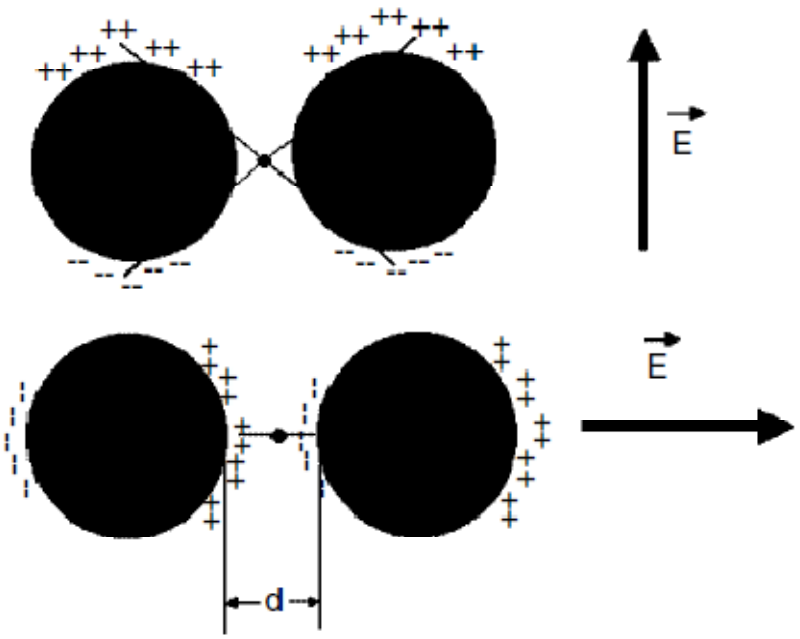

Fig 5.1 Effect of polarized light along the interparticle axis and across the axis

in the interstice between two metal nanospheres is flanked by two sets of (time-varying) conjugate charges arising from polarization of the individual nanoparticles. (The model also describes the two-dimensional component of any system through which a planar cut is represented by two circles, as for example for two parallel nanowires.) As the nanoparticles are brought closer together, the proximity of these charges to the molecule can be made arbitrarily close and hence the capacitive field sensed by the molecule commensurately large. The mutual interaction of the two nanospheres (or nanowires) also leads to an increase in the magnitude of the dipole induced in each component of the two-component nano-system. The dipole induced in each nano-object arises from the combined field of the incident light and the intense field of its partner, which, in this configuration, leads to an amplification of the polarization. If this problem is solved

naively as one of simple electrostatics involving two polarizable nanoparticles, then for light polarized along the inter-particle axis the enhancement increases approximately as d^{-8} where *d* is the gap size between the two nanowires.

In contrast, if the light is polarized in the other direction illustrated in Fig.5.1 (top), i.e. normal to the axis joining the centers of the two nanospheres, a molecule in the interstitial region will not benefit from proximity to the induced charges, however closely the nanoparticles are brought together. Nor is there any other location where the field benefits distinctly from the fact that one has a system of two particles rather than one. Additionally, the mutual polarization of each of the two nanoparticles as a result of the field emitted by the other is not favorable.

Bringing two particles together also brings about other effects that one needs to be mindful of, for example, the plasmon resonance splits into two polarization-sensitive components[34], one of which has a resonance that depends strongly on the separation of the two nanospheres. Hence, as the two nanoparticles are separated, the SERS enhancement will diminish and the resonance condition will change simultaneously.

Further aggregation into larger clusters will create opportunities for other 'hot' interstitials, each of which will have its own characteristics of polarization and field strength.

The precise structure of the nanoparticle cluster has yet another important aspect. For highly (geometrically) symmetric aggregates, the degeneracies of the normal modes describing the surface plasmon excitations will be such that they will be characterized generally by relatively narrow excitation spectra, whereas clusters with lower geometrical

symmetries will have much broader excitation spectra. This will strongly affect resonance conditions.

Nanoparticle aggregates grown by self-assembly from monomers in solution often show scaling symmetry either as self-similar or (when deposited on a substrate) self-affine systems. The exciting field does not possess scaling symmetry while the cluster does, a form of energy localization arises that can lead to the formation of electromagnetic hot spots with field strengths that are often of the same magnitude as those discussed above for the nanoparticle dimer. However the lack of translational symmetry in the nanoparticle leads to formation of broad spectra.

There are other electromagnetic mechanisms that can augment the SERS enhancement. Prime among them is the creation of structures such as ellipsoids and nanowires with regions of very large curvature[35]. This is known as the lightening rod effect.

5.3 Influence of geometry on intense SERS

Consider an oxide-covered silicon surface derivatized with 3-aminopropyltrimethoxysilane to discourage the nanoparticles from diffusing and aggregating. The surface was only sparingly covered with silver nanoparticles[36]. Excess nanoparticles were washed off and the silver was exposed to a solution of 1, 4-benzenedithiol, a rigid molecular linker that, in principle, can connect two silver nanoparticles together by making a bond to each using its thiol functional groups. Raman spectra were recorded at this step. The sample was then exposed to a second dosing of silver nanoparticles in the hope that the nanoparticles would bind to the dangling sulfur

functionalities already present on the Ag particles decorating the surface. Raman spectra were once again recorded. The process is illustrated in Fig. 5.2.

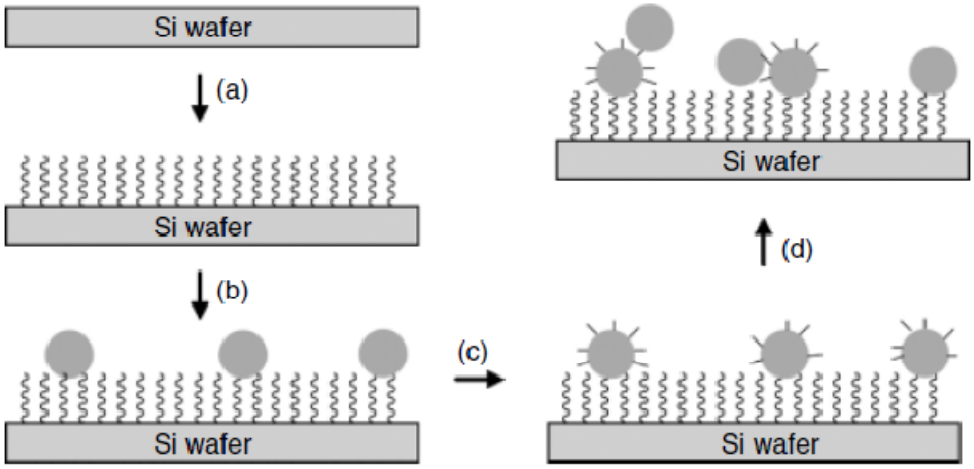

Fig 5.2 self assembly of linker bonded silver nanospheres clusters

The effect on the SERS spectra of linking silver nanoparticles is dramatic (Fig. 5.2a). Before step d (the second dosing with silver nanoparticles) was carried out, the sample showed primarily the Raman spectrum of the Si substrate [although very occasionally a weak Raman feature belonging to the dithiol is observed; Fig. 5.2(b)]. When a second dosing with silver nanoparticles was carried out, one found many small clusters on the surface that showed intense SERS signals belonging to the dithiol [Fig. 5.2(c)]. In a control experiment in which the aggregate amount of silver deposited in the two silver dosings was placed on the substrate in the first dose, no significant increase in SERS intensity or in the number of SERS-active clusters was observed. The straightforward explanation for these observations is that the nanoparticles self-assemble into small clusters under the influence of the dithiol linkers. More to the point, the nanoparticle clusters are assembled with the appropriate geometry for super-intense SERS, namely

closely coupled particles with very narrow interstices and with the dithiol automatically positioned at the SERS hot spots. The occasional observation of weak SERS before the addition of the second layer of silver nanoparticles is presumably due to the occasional incorporation of the dithiol at the right location within clusters formed accidentally (and therefore far less frequently) with the required inter-particle geometry.

Using this stepwise assembly process guarantees that almost every cluster formed in step d becomes a hot particle, while pre-forming clusters then adsorbing dithiol on them rarely produce hot clusters, as was observed in most of the early reports of single-molecule SERS. The results demonstrate the strong influence of geometry on intense SERS.

5.4 Influence of polarization on SERS intensity

In order to study the effect consider the experiment done with Silver nanowires grown in highly ordered porous anodic alumina (PAO) templates, electrochemically fabricated in 0.3M oxalic acid using the two-step anodization process reported by Masuda and Fukuda [56]. Silver metal deposition was carried out at room temperature by AC electrolysis in a 0. 05M $AgNO_3$ electrolyte. On average, the silver nanowires so fabricated were 35 nm in diameter and 10 μm in length. Silver nanowires were released from the oxide templates by etching, ultrasonically dispersed in methanol and deposited out of solution on a pre-cleaned oxide-covered silicon wafer. Rhodamine 6G dye (R6G) adsorbate was applied to the SERS substrate out of a very dilute methanol solution.

A large number of flat nanowire bundles that retained their parallel alignment, presumably as a result of van der Waals' interactions, were found in the deposit. Laser

excitation of R6G-dosed silver nanowire rafts produced intense SERS spectra. The spectra agree well with those reported by others. Surface-enhanced Raman spectroscopy intensity maps of a section of a nanowire raft were produced by selecting a 38x32μm^2 rectangular area and then recording the SERS spectrum at 0.5μm intervals. The SERS intensity maps were created by plotting the (baseline corrected) intensity of the 1649 cm^{-1} line of R6G excited with 514.5 nm argon ion laser light (obtained with two orthogonal polarizations). The polarization was rotated using a half-wave plate placed before the sample. No cross-polarizer was used after signal collection.

The polarization dependence is striking and in keeping with theory. For an aligned system of nanowires there are, in principle, six combinations of combined $\boldsymbol{E}$ and $\boldsymbol{k}$ vector directions possible. With the experimental configuration used by them only two are accessible. The first corresponds to the electric vector lying across the long axes of the nanowires and in the plane of the nanowires. The second has the electric vector in the plane of the nanowires but aligned along their long axes. We will call the first 'across the nanowires'. It was argued above to be the most favorable condition for observing strong SERS, as is, indeed, what is observed. Light polarized across the nanowires produces a SERS signal that, on average, is approximately tenfold more intense than what is observed with light polarized along the nanowires.

The polarization effect illustrates the strong and localized enhancement of the electromagnetic field possible at favorable locations (such as the interstitial gap between the nanowires) in systems of interacting nanostructures. The reason why the experimental SERS intensity ratio is only a factor of ten (whereas theory predicts factors of four or five orders of magnitude) can be readily understood. First, the nanowires in the raft are not

ideally parallel, and even a slight departure from ideal parallelism can result in a significant increase in intensity for polarizations nominally along the nanowires. Second, the enhancement for light polarized across the nanowires is not expected to be as great (per molecule) for a system of many parallel nanowires as for a single pair. Finally, the laser light is not ideally polarized as a result of focusing by a small numerical aperture lens that produces a component of orthogonally polarized light along with the desired component. Hence, the SERS signal excited with light polarized along the nanowires is very much more intense than it would ideally be.

CHAPTER 6

EXPERIMENTAL RESULTS

6.1 Instruments Used

1) SERS: Backscattered Raman spectra were recorded using a LabRam microRaman system (Jobin-Yvon/ISA) equipped with a thermoelectrically cooled CCD detector. The lens magnification used (50X). He-Ne laser of wavelength 785 nm is used. The exposure time is 20s
2) SEM Imaging : Jeol JSM 7500F FESEM
3) ALD : Cambridge Nanotech Inc's Savannah S100
4) Electroplating : (i) Bk precision 1787B 0-72V/0-1.5A single o/p programmable DC power supply

   (ii) Ceramag M1D1/IKA Works Hot plate stirrer

   (iii) Elma Ultrasonic vibrator
5) Sputtering : SPI module sputter coater with SPI module control.

6.2 SERS spectra of 4-Mercaptopyridine

4-Mercapto pyridine solution $(10^{-3}M)$ is prepared by using ethanol. When a drop of the solution is placed on the SERS substrate the ethanol evaporates leaving behind 4-Mercapto pyridine molecules.

Copper nanowires decorated by gold nanoparticles are used as the SERS substrate. The excitation wavelength used is 784.9 nm. Copper nanowires have a plasmon resonance of 560 nm and gold nanoparticles have a plasmon resonance of 520nm. The effective plasmon resonance is influenced by the copper nanowires, gold nanoparticles,

Silicon wafer and the air. The plasmon resonance does shift to higher wavelengths. The main reason for enhancement is electromagnetic coupling between the copper nanowires and gold nanoparticles

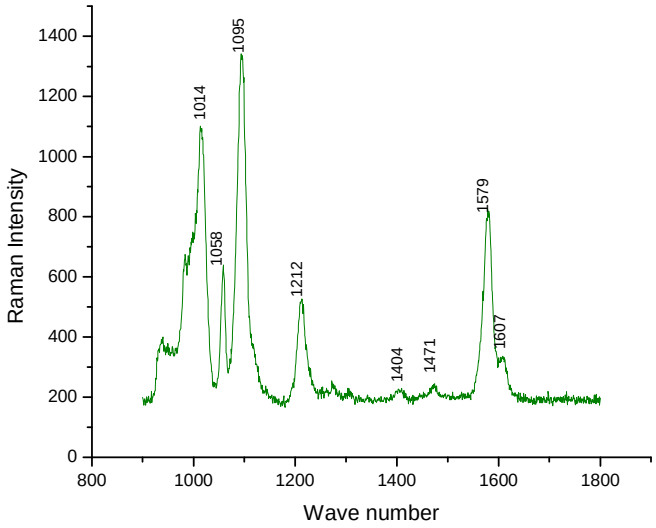

Fig 6.1 Peak assignments for raman spectra of 4Mpy molecule

The spectrum consists of several peaks at 1014, 1058, 1095, 1212, 1579 cm^{-1}which are intrinsic to 4-Mpy. The band at 1212 $cm^{-1}$is attributed to in plane N-H deformation and the band at 1095 cm^{-1} arises from the ring breathing mode that is coupled with C-S stretching. Furthermore the bands at 1579 and 1014 cm^{-1} may be assigned to ring stretching mode and ring breathing vibration mode of adsorbed 4Mpy (4 Mercaptopyridine).

Mpy solution	Cu NW-Au NP	Assignment
998		Ring breathing
1049	1014	$\beta(CH)$
	1058	$\beta(CH)$
1119	1095	Ring breathing/C-S
	1212	$\beta(CH)$/NH
1255		$\beta(CH)$
1283		$\beta(CH)$
1487		$\upsilon(C=C\ /\ C=N$
1585	1579	$\upsilon(CC)$
1618		$\upsilon(CC)$

.

Table 6.1 Raman peak assignments[37]

6.3 SEM Images of Copper nanowires

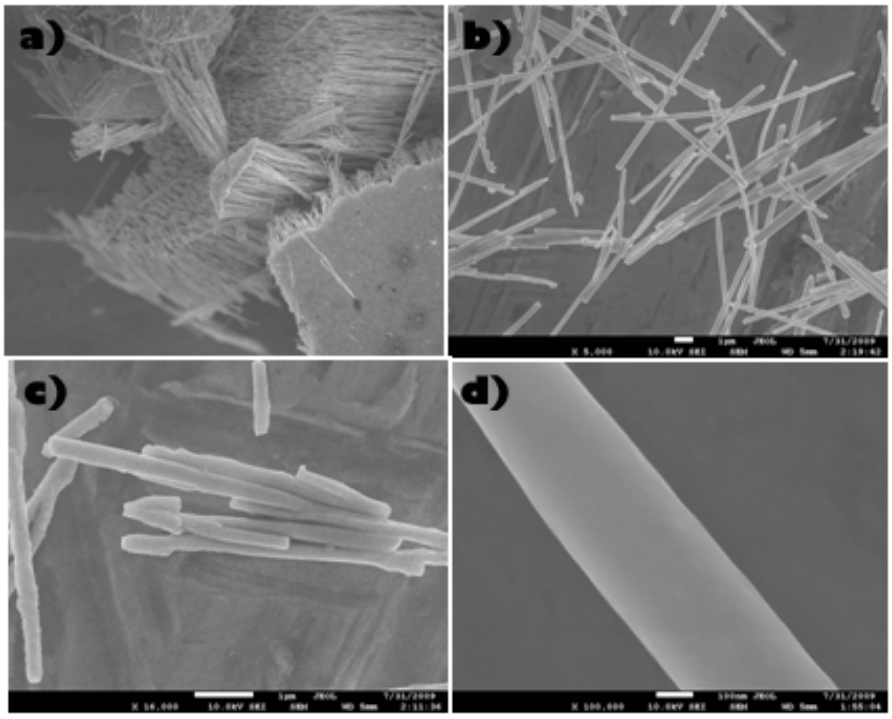

Fig 6.2a) Cu nanowires attached to a thin Cu film b) &c) NW aggregates d) single NW

The copper nanowires have a diameter of 200nm, same as the diameter of the holes in the anodisc used. As the deposition time is increased (~60-80 min) a thin layer of copper is formed holding the nanowires together as seen in fig 6.2a.

6.4 SEM Images of Copper Nanowires decorated with Gold Nano particles

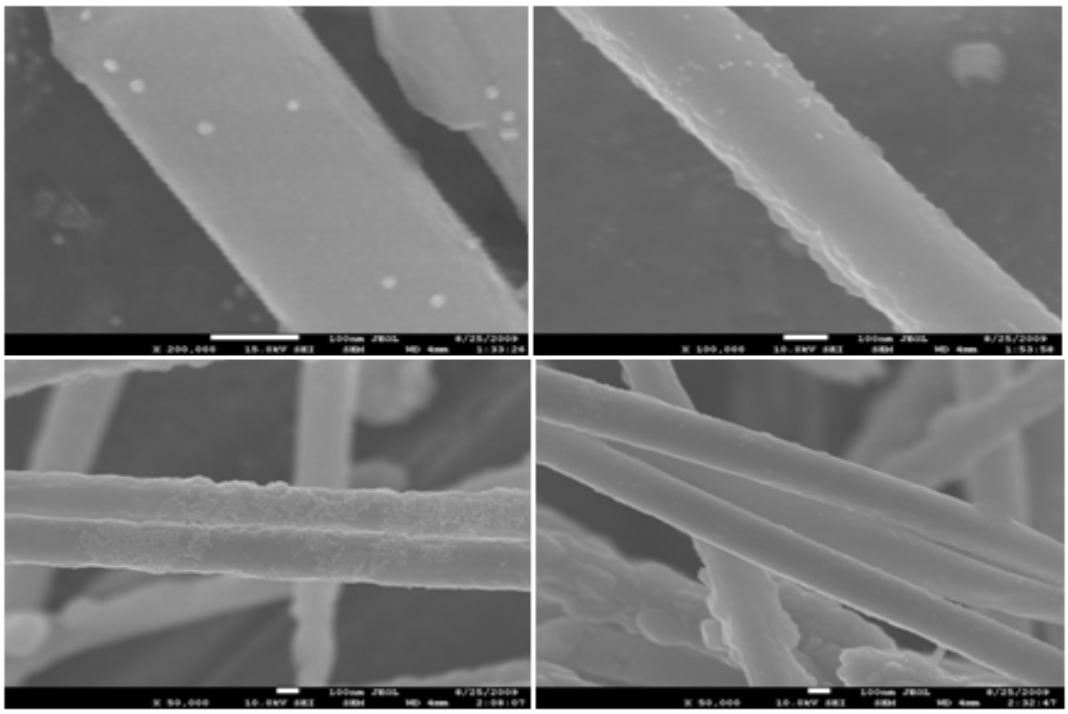

Fig 6.3 Cu nanowires decorated by gold nanoparticles

The gold nanoparticles deposited on the copper nanowire were not uniform along the length of the nanowire. When several nanowires were stocked up the gold nanoparticles mostly were deposited on the top layer and very few on the layers below. As the nanowires have a higher diameter of 200 nm most of the gold nanoparticles lied on the Silicon wafer.

6.5 SERS results of 4-mercapto pyridine molecule

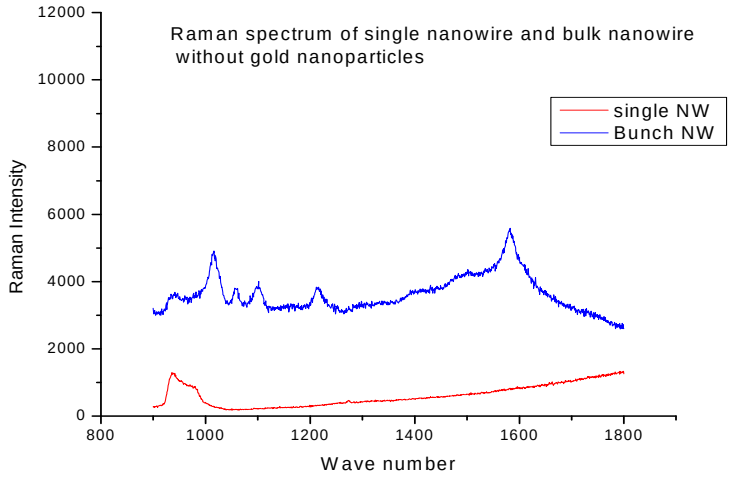

Fig 6.4 RS of single NW and bunch of NW without gold nanoparticles

The signal from single nanowire has no strong peaks while the spectrum from bulk nanowires has strong peaks. This is due to the enhancement obtained by the electromagnetic coupling between the copper nanowires

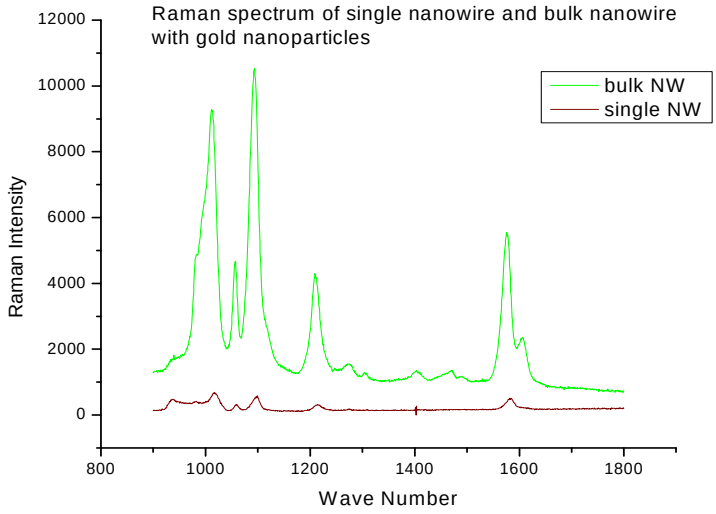

Fig 6.5 RS of single NW and bunch of NW with gold nanoparticles

The bulk nanowire has strong peaks than single nanowire as there is stronger coupling at the junction when two nanowires meet or overlap. The formation of these junctions cannot be controlled hence we prefer the coupling of the nanowire-nanoparticle than the coupling of nanowire-nanowire junction.

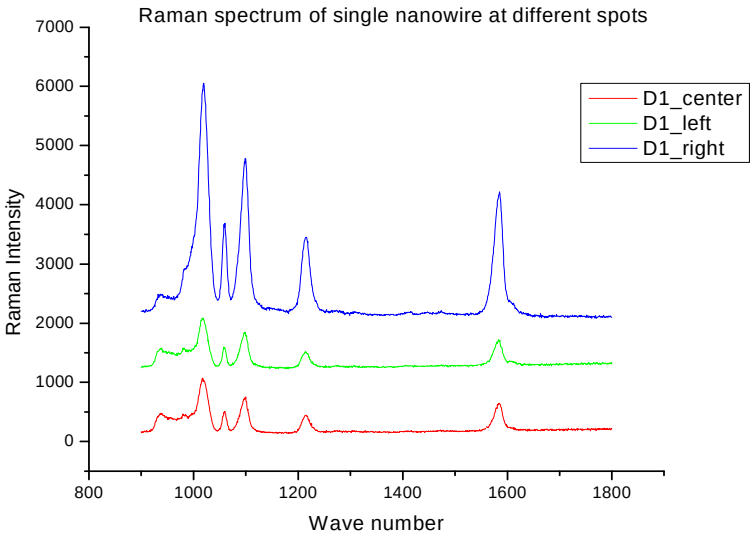

Fig 6.6 Raman spectrum of single nanowire at different points

The intensity is different at each point because there is no uniform distribution of the gold nanoparticles over the nanowire the surface plasmon resonance can be slightly different at each point. In case of uniform distribution of nanoparticles, the symmetry would render the point polarization independent.

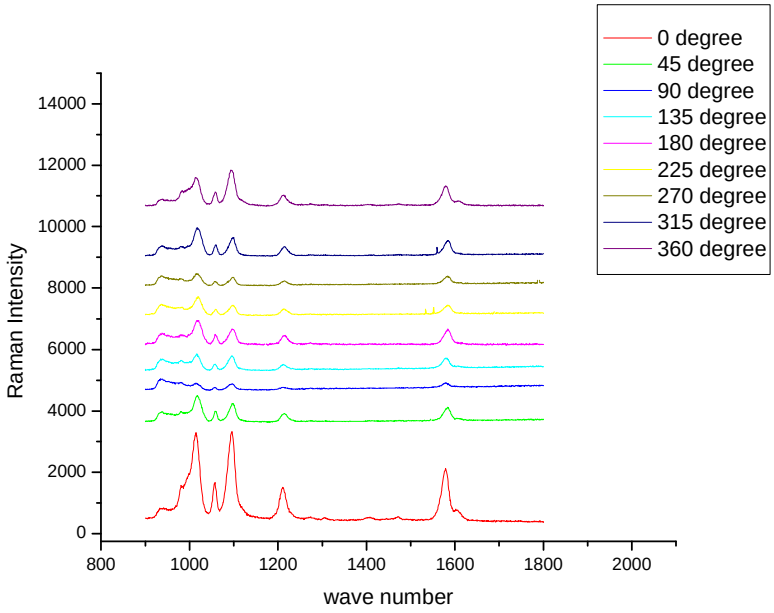

Fig 6.7 RS of single nanowire at different polarization angles

The nanoparticle-nanowire system does not have a polarization effect similar to the dimer because in a dimer there is only one interparticle axis while in the case of the nanoparticle-nanowire system the nanoparticle can interact along several nanoparticle-nanowire axes.

The angle θ is the angle between the normal to the nanowires long axis and the incident field polarization ‘p’

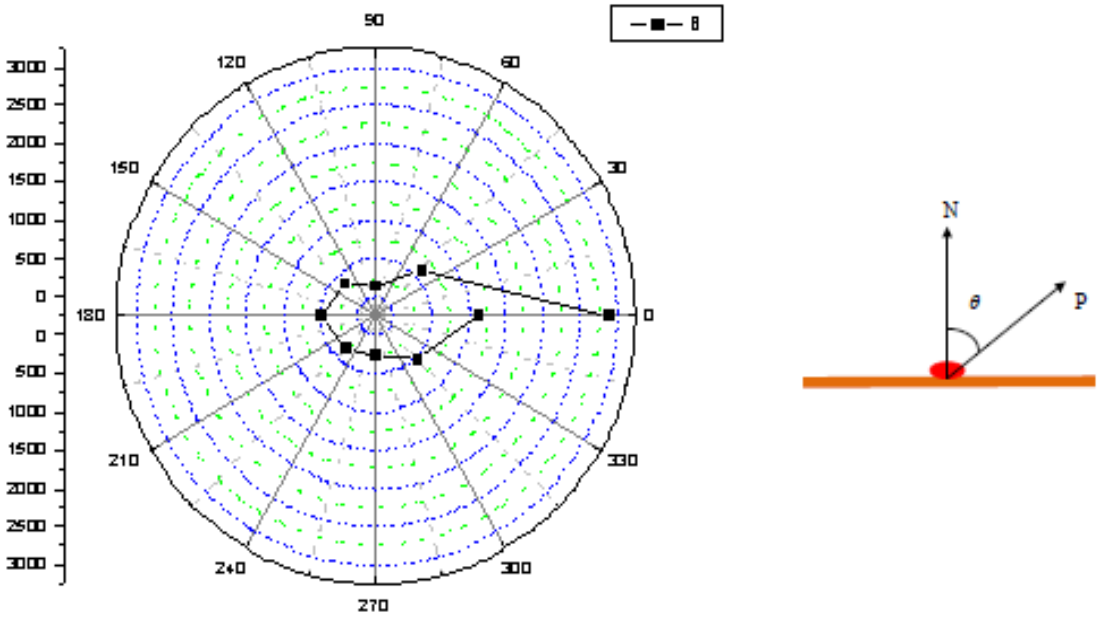

Fig 6.8 polar plot of the polarization dependent SERS at 1094cm^{-1}

All the major raman bands of 4-mercapto pyridine showed similar polarization angle dependence.

6.6 SERS results of pyridine molecule after ALD

The idea was to decrease the pore size of the anodisc by using ALD thereby we can get thin copper nanowires and observe the size dependence of the nanowires on the signal enhancement. A thin film of aluminum oxide was coated uniformly over it but the diameter of the nanowires did not improve, only the length of the nanowires improved.

6.7 Conclusion and Future Experiments

Copper nanowires decorated by gold nanoparticles serve as a good SERS substrate for the detection of 4 mercapto pyridine molecule ($10^{-3}M$) for laser excitation wavelength at 784.9 nm. The normal SERS substrates made of gold and silver are costly compared to the one with copper. The effects are accounted for in terms of electromagnetic fields concentrated in hotspots at the NW-NP junction.

The spectral features observed agree well with those reported previously for 4-mercapto pyridine.

The future work can be concentrated on :

a) We do not know exactly how many molecules are transferred on to the substrate as making an estimate of the molecules transferred is extremely difficult. If we can control the molecules transferred our results will be more precise and reproducible.

b) If we can get the uniform deposition of gold nanoparticles onto the Copper nanowires (try to use physical or chemical methods)

REFERENCES

1. http://en.wikipedia.org/wiki/Anodizing.

2. http://www.whatman.com/PRODAnoporeInorganicMembranes.aspx.

3. http://www.ajaint.com/whatis.htm.

4. http://www.2spi.com/catalog/manuals/SputterModuleManual.pdf.

5. http://electrochem.cwru.edu/encycl/art-e01-electroplat.htm.

6. McFarland AD, Haynes CL, Mirkin CA, Van Duyne RP, Godwin HA. Color My Nanoworld W. *Issues*. 2004.

7. Wang Z, Pan S, Krauss TD, Du H, Rothberg LJ. The structural basis for giant enhancement enabling single-molecule Raman scattering. *Proc Natl Acad Sci U S A*. 2003;100(15):8638. http://ezproxy.library.unlv.edu/login?url=http://search.ebscohost.com/login.aspx?direct=true&db=aph&AN=10524534&site=ehost-live.

8. http://en.wikipedia.org/wiki/Atomic_Layer_Deposition.

9. sami f. *Introduction to Micro Fabrication.* ; 2004.

10.http://cambridgenanotech.com/cnpruploads/Cambridge%20NanoTech%20Web%20Overview.pdf.

11. Raman C, Krishnan K. A new type of secondary radiation. *Nature*. 1928;121(3048):501.

12. bubert H, Jenett H. wiley-vch; 2002.

13. Nie S, Emory SR. Probing single molecules and single nanoparticles by surface-enhanced Raman scattering. *Science*. 1997;275(5303):1102. http://search.ebscohost.com/login.aspx?direct=true&db=aph&AN=9703135262&site=ehost-live.

14. Fleischmann M, Hendra P, McQuillan A. Raman spectra of pyridine adsorbed at a silver electrode. *Chemical Physics Letters*. 1974;26:163-166.

15. Jeanmaire DL, Van Duyne RP. Surface Raman spectroelectrochemistry. Part I. Heterocyclic, aromatic, and aliphatic amines adsorbed on the anodized silver electrode. *J Electroanal Chem*. 1977;84(1):1-20.

16. Albrecht MG, Creighton JA. Anomalously intense Raman spectra of pyridine at a silver electrode. *J Am Chem Soc*. 1977;99(15):5215-5217.

17. Tian Z, Ren B, Mao B. Extending surface Raman spectroscopy to transition metal surfaces for practical applications. 1. Vibrational properties of thiocyanate and carbon monoxide adsorbed on electrochemically activated platinum surfaces. *J Phys Chem*. 1997;101(8):1338-1346.

18. Smith E, Dent G. *Modern Raman spectroscopy: a practical approach.* Wiley; 2005.

19. Campion A, Kambhampati P. Surface-enhanced Raman scattering. *Chem Soc Rev*. 1998;27(4):241-250.

20. Creighton JA, Eadon DG. Ultraviolet–visible absorption spectra of the colloidal metallic elements. *Journal of the Chemical Society, Faraday Transactions*. 1991;87(24):3881-3891.

21. Langhammer C, Yuan Z, Zoric I, Kasemo B. Plasmonic properties of supported Pt and Pd nanostructures. *Nano Lett*. 2006;6(4):833-838.

22. Eric LR, Etchegoin P. *principles of surface enhanced raman spectroscopy and related plasmonic effects*. Elsemier; 2009.

23. Mock JJ, Barbic M, Smith DR, Schultz DA, Schultz S. Shape effects in plasmon resonance of individual colloidal silver nanoparticles. *J Chem Phys*. 2002;116(15):6755. http://search.ebscohost.com/login.aspx?direct=true&db=aph&AN=6426998&site=ehost-live.

24. Kneipp H, Moskovits M. *Surface-enhanced raman scattering: physics and applications.* Springer Verlag; 2006.

25. Moskovits M, Suh J. Surface selection rules for surface-enhanced Raman spectroscopy: calculations and application to the surface-enhanced Raman spectrum of phthalazine on silver. *J Phys Chem*. 1984;88(23):5526-5530.

26. Michota A, Bukowska J. Surface-enhanced Raman scattering (SERS) of 4-mercaptobenzoic acid on silver and gold substrates. *J Raman Spectrosc*. 2003;34(1).

27. mick w, kamali k, geoff s, michelle s, burkhard r. *nanotechnology basic science and emerging technologies.* chapman and hall; 2002.

28. Alarie J, Stokes D, Sutherland W, Edwards A, Vo-Dinh T. Intensified charge coupled device-based fiber-optic monitor for rapid remote surface-enhanced Raman scattering sensing. *Appl Spectrosc*. 1992;46(11):1608-1612.

29. Taranenko N, Alarie JP, Stokes DL, Vo-Dinh T. Surface-enhanced Raman detection of nerve agent simulant (DMMP and DIMP) vapor on electrochemically prepared silver oxide substrates. *J Raman Spectrosc*. 1996;27(5):379-384.

30. Han XX, Zhao B, Ozaki Y. Surface-enhanced Raman scattering for protein detection. *Analytical & Bioanalytical Chemistry*. 2009;394(7):1719-1727. http://ezproxy.library.unlv.edu/login?url=http://search.ebscohost.com/login.aspx?direct=true&db=aph&AN=43169031&site=ehost-live. 10.1007/s00216-009-2702-3.

31. Stuckless JT, Moskovits M. Enhanced two-photon photoemission from coldly deposited silver films. *Physical Review B*. 1989;40(14):9997-9998.

32. Shalaev VM, Douketis C, Haslett T, Stuckless T, Moskovits M. Two-photon electron emission from smooth and rough metal films in the threshold region. *Physical Review B*. 1996;53(16):11193-11206.

33. Xu H, Kall M. Estimating SERS properties of silver-particle aggregates through generalized Mie theory. *TOPICS IN APPLIED PHYSICS*. 2006;103:87.

34. Aravind P, Nitzan A, Metiu H. The interaction between electromagnetic resonances and its role in spectroscopic studies of molecules adsorbed on colloidal particles or metal spheres. *Surf Sci*. 1981;110(1):189-204.

35. Wang DS, Kerker M. Absorption and luminescence of dye-coated silver and gold particles. *Physical Review B*. 1982;25(4):2433-2449.

36. Moskovits M, Jeong DH. Engineering nanostructures for giant optical fields. *Chemical Physics Letters*. 2004;397(1-3):91-95.

37. Wang Y, Hu H, Jing S, et al. A SPECIAL ISSUE ON ADVANCED VIBRATIONAL SPECTROSCOPY--FROM NEAR-INFRARED TO TERAHERTZ-Enhanced Raman Scattering as a Probe for 4-Mercaptopyridine Surface-modified Copper Oxide Nanocrystals. *Analytical Sciences*. 2007;23(7):787-792.

VITA

Graduate College
University of Nevada, Las Vegas

Roshan Guttikonda

Degree:

Bachelor of Technology, Electronics and Communication Engineering, 2007
Acharya Nagarjuna University, Guntur, India

Thesis Title: Individual Copper Nanowire Decorated by Gold Nanoparticles for Surface Enhanced Raman Scattering

Thesis Examination Committee:

Chairperson, Biswajit Das, Ph.D, P.E.
Committee Member, Yingtao Jiang, Ph.D
Committee Member, Mei Yang, Ph.D
Graduate Faculty Representative, Laxmi P. Gewali, Ph.D